

## **Response to Reviewers**

We appreciate the two anonymous reviewers for their constructive criticisms and valuable comments, which were of great help in improving the quality of the manuscript. We have revised the manuscript accordingly and our detailed responses are shown below. All the revision is highlighted in the revised manuscript.

Interactive comment on “Sources of volatile organic compounds and policy implications for regional ozone pollution control in an urban location of Nanjing, East China” by Qiuyue Zhao et al.

### **Anonymous Referee #2**

In this study, the authors conducted one-year VOC observation at an urban site in Nanjing. They analyzed the seasonal and diurnal characteristics of 56 VOCs as well as their sources using the PMF model. A box model together with a Master Chemical Mechanism (MCM) was used to identify the relationships between the contributions of VOC sources and the O<sub>3</sub> formation. The results were also compared with VOCs data from other Chinese megacities like Beijing, Guangzhou, and Shanghai. VOC have been well recognized to be responsible for the swift development of air pollution events since volatile organic compounds are key precursors of O<sub>3</sub> and secondary organic aerosols (SOA). However, the speciation and emission strength of these VOC have been demonstrated to be hard to acquire due to the fact that VOC can be emitted from a diversity of domestic and industrial activities. Therefore, measurements of VOC emissions are critically needed in China. This work can be a significant contribution to the atmospheric research community. Overall, the manuscript is fairly well written and I would recommend the manuscript for publication after minor revisions.

Reply: We highly appreciate the reviewer’s positive comments and helpful suggestions. We have addressed all the comments/suggestions in the revised manuscript. Detailed responses to the individual specific comment/suggestion are as follows.

**Specific concerns:**

1. Line 61: What's "photochemical industry"?

Reply: Sorry for the mistake. It should be "petrochemical industry". For details, please refer to Line 62, page 2 in the revised manuscript.

2. Sample location: there is always an asphalt waterproof layer on the rooftop of an office building. How to avoid the interference of this emissions?

Reply: We thank the reviewer's valuable comment. There is a waterproof layer on the rooftop of the building but there was no guarantee that it was made of asphalt. Furthermore, despite this waterproof layer on the rooftop of the building, the interferences of emissions from this layer were believed to be insignificant because: 1) The waterproof layer was covered by the layer of concrete, which was further covered with a layer of ceramic tile; 2) The building had been built for three years before the sampling campaign was started; 3) It was documented that the VOC emitted from asphalt mainly included benzene, toluene, ethylbenzene and xylene. However, the levels of benzene, toluene, ethylbenzene, m/p-xylene and o-xylene were lower than those observed in other urban, industrial and rural environments in different regions (section 3.1, He et al., 2019; Mo et al., 2015, 2017; An et al., 2014 and 2015; Zhang et al., 2012). 4) The sampling inlet was about 2-3 m above the rooftop of the building. Indeed, there is a waterproof layer on the rooftop of building. Therefore, we believe that though there is a waterproof layer for the rooftop of the building, the interference of its emission on ambient VOCs was insignificant.

The above text has been added in the revised manuscript to highlight the insignificant influence of waterproof layer on the rooftop of the building

For details, please refer to Lines 88-97, Page 3 in the revised manuscript.

**Reference:**

- Gardiner, M.S., Lange, C.R., 2005. Comparison of laboratory generated and field-obtained HMA VOCs with odour potential. *The International Journal of Pavement Engineering* 6, 257-263.
- He Zhuoran, et al., 2019. Contributions of different anthropogenic volatile organic compound sources to ozone formation at a receptor site in the Pearl River Delta region and its policy implications. *Atmospheric Chemistry and Physics* 19, 8801-8816.

Zhang, Y.L., Wang, X.M., Blake, D.R., Li, L.F., Zhang, Z., Wang, S.Y., Guo, H., Lee, F.S.C., Gao, B., Chan, L.Y., Wu, D., Rowland, F.S., 2012. Aromatic hydrocarbons as ozone precursors before and after outbreak of the 2008 financial crisis in the Pearl River Delta region, south China. *Journal of Geophysical Research* 117, D15306, doi:10.1029/2011JD017356.

3. Aromatics are important of gasoline. So, source 5 could be identified as gasoline cars. Thus, the identification of source 5 to industrious emissions may be need more relevant tracers.

Reply: The reviewer's valuable comment is highly appreciated. We agreed with the reviewer that aromatic hydrocarbons, especially benzene, toluene, ethylbenzene and xylenes could also emitted from gasoline vehicles. However, in addition to gasoline vehicle emissions, industrial emission could be another important contributor to ambient aromatic hydrocarbons in the Yangtze River Delta, Pearl River Delta and North China Plain (Yuan et al., 2009; He et al., 2019; Zhang et al., 2013, 2014; Mo et al., 2015, 2017; An et al., 2014). The tunnel studies and emission-based measurement results found that aromatic hydrocarbons from gasoline vehicle exhaust were coherently emitted with pentanes, butenes, *n*-hexane, and cyclopentane, which were more consistent with the profile in source 3 mentioned above (Liu et al., 2008; Ho et al., 2009; Yuan et al., 2009; Zhang et al., 2018). Therefore, the absence of above species in source 5 indicated that this source could be related to industrial emission (Zhang et al., 2014). Particularly, the high presence of toluene, ethylbenzene, xylenes, ethyltoluene and trimethylbenzene was consistent with the emission-base measurement results conducted in paint and printing industries (Yuan et al., 2010) and manufacturing facilities (Zheng et al., 2013). On the other hand, the profile of high presence of aromatic hydrocarbons ( $C_7$ - $C_9$  aromatics) and the certain amount of ethene, was also agree with the profiles measured in the areas dominated by industrial emissions in the Yangtze River Delta region (An et al., 2014; Shao et al., 2016; Mo et al., 2017). For example, An et al. (2014) reported that toluene, ethylbenzene, xylenes, and trimethylbenzenes could be emitted from different industrial processes, and identified that the factors with high loadings of these species as industrial production, solvent usage and industrial production volatilization sources by PAC/APCS at the industrial

area in Nanjing. On the other hand, Mo et al. (2017) identified the factors with high concentrations of C<sub>7</sub>-C<sub>9</sub> aromatics and ethene as residential solvent usage, chemical and paint industries and petrochemical industry with the PMF model applied to the data collected in an industrialized coastal city of Yangtze River Delta region. To further identify source 3 and source 5, the ratio of toluene/benzene (T/B, ppbv/ppbv) in each profile was compared with those obtained from emission-based measurements and tunnel study results (Zhang et al., 2018 and references therein). The ratios of T/B were ~8.2 and ~1.2 for sources 5 and 3, respectively, and were consistent with those of “industrial processes and solvent application”, and “roadside and tunnel study”, respectively (Zhang et al., 2018 and references therein). This further confirmed that source 3 was related to gasoline vehicular exhaust, while source 5 was associated with industrial emission.

The above discussion has been provided in the revised manuscript to further clarify source 5 and source 3. For details, please refer to Lines 407-440, Pages 14-15 in the revised manuscript.

### References:

- Ho, K.F., et al., 2009. Vehicular emission of volatile organic compounds (VOCs) from a tunnel study in Hong Kong. *Atmospheric Chemistry and Physics* 9, 7491-7504.
- Liu, Y., et al., 2008. Source apportionment of ambient volatile organic compounds in the Pearl River Delta, China: Part II. *Atmospheric Environment* 42, 6261-6274.
- Shao, P., An, J.L., Xin, J.Y., Wu, F.K., Wang, J.X., Ji, D.S., Wang, Y.S., 2016. Source apportionment of VOCs and the contribution to photochemical ozone formation during summer in the typical industrial area in the Yangtze River Delta, China. *Atmospheric Research* 176-177, 64-74.
- Yanli Zhang, et al., 2013. Species profiles and normalized reactivity of volatile organic compounds from gasoline evaporation in China. *Atmospheric Environment* 79, 110-118.
- Yuan, B., Shao, M., Lu, S.H., Wang, B., 2010. Source profiles of volatile organic compounds associated with solvent use in Beijing, China. *Atmospheric Environment* 44, 1919-1926.
- Zhang Yanli, et al., 2018. Decadal changes in emissions of volatile organic compounds (VOCs) from on-road vehicles with intensified automobile pollution control: case study in a busy urban tunnel in south China. *Environmental Pollution* 233, 806-819.
- Zheng, J.Y., Yu, Y.F., Mo, Z.W., Zhang, Z., Wang, X.M., Yin, S.S., Peng, K., Yang, Y., Feng, X.Q., Cai, H.H., 2013. Industrial sector-based volatile organic compound (VOC) source profiles measured in manufacturing facilities in the Pearl River Delta, China. *Science of the Total Environment* 456-457, 127-136.
- Zibing Yuan, et al., 2009. Source analysis of volatile organic compounds by positive matrix factorization in urban and rural environments in Beijing. *Journal of Geophysical Research* 114,

4. Why the diurnal trend of fuel evaporation showed a decrease at noon time since this source is temperature dependent?

Reply: Thanks a lot for the comment. Apart from emissions, ambient VOC concentrations are largely determined by photochemistry and dilution processes, in particular the variations of mixing height in the course of a day (Gillman et al., 2009; Wang et al., 2013). Though the evaporation of fuel is dependent on temperature, the average temperature in the morning and evening (*i.e.*, 0800-1000 and 1700-1900 LT, respectively) when peaks of fuel evaporation were found was only about  $\sim 1.2$  °C lower than that observed from noon to afternoon (1100-1600 LT), which may not result in much higher fuel evaporation at noon (the difference between maximum and minimum values for fuel evaporation was found to be  $\sim 6$   $\mu\text{g}/\text{m}^3$ ). On the other hand, in addition to evaporation from the gas station, fuel could evaporate from hot engines, fuel tanks and the exhaust system when the car is running. Furthermore, the engine remains hot for a period of time after the car is turned off, and gasoline evaporation continues when the car is parked (Technology center, University of Illinois, <https://mste.illinois.edu/tcd/ecology/fuelevap.html>, access date: 25 December 2019). The similarity of diurnal variations of fuel evaporation to vehicular emissions suggested that the prominent peak in the morning and evening hours were related to the increased vehicles in the traffic rush hour and emissions accumulated in the relatively low boundary layer.

To provide detailed discussion on the diurnal pattern of fuel evaporation, the above analysis text has been added in the revised manuscript. For details, please refer to Lines 490-501, Page 17 in the revised manuscript.

## References

- Gilman, J.B., Kuster, W.C., Goldan, P.D., Herndon, S.C., Zahniser, M.S., Tucker, S.C., Brewer, W.A., Lerner, B.M., Williams, E.J., Harley, R.A., Fehsenfeld, F.C., Warneke, C., de Gouw, J.A., 2009. Measurements of volatile organic compounds during the 2006 TexAQS/GoMACCS campaign: industrial influences, regional characteristics, and diurnal dependencies of the OH reactivity. *Journal of Geophysical Research* 114, D7, doi: 10.1029/2008JD011525.

Wang, H.L., Chen, C.H., Wang, Q., Huang, C., Su, L.Y., Huang, H.Y., Lou, S.R., Zhou, M., Li, L., Qiao, L.P., Wang, Y.H., 2013. Chemical loss of volatile organic compounds and its impact on source analysis through a two-year continuous measurement. *Atmospheric Environment* 80, 488-498.

### **Anonymous Referee #1**

Zhao et al. describe VOC measurements conducted at the Jiangsu Academy of Environmental Science (JAES) in Nanjing, China. The authors measure VOCs using a GC system, and interpret the sources of these VOCs using positive matrix factorization. The authors evaluate the environmental impacts of these emissions on ozone formation using an observation-based model (OBM) employing the Master Chemical Mechanism (MCM v3.2), and identify the anthropogenic VOCs likely to be significant ozone precursors. The authors also evaluate ozone sensitivities to VOC and NO<sub>x</sub> reductions, and conclude that VOC reductions would be the best strategy to reduce ozone in Nanjing.

In general, the manuscript reads very well and is well-organized to tell a coherent message. I appreciate the authors work to carefully measure VOCs and benchmark these measurements against other cities in China. I am generally convinced by the PMF results given that the authors interpretation is reasonable, and the PMF factors are prescribed to obvious sources in the Nanjing area (which are very well described); however, I do have some recommendations that could improve the PMF analysis and strengthen the justification of source apportionment. Finally, I believe the use of the OBM is justified to evaluate VOC RIR, but I am not convinced that the OBM can be used to evaluate the ozone isopleth without further evidence that the model is doing an adequate job to capture ozone formation in the Nanjing region. My comments below primarily address PMF and the OBM.

[Reply: Thanks for the reviewer's positive comments and helpful suggestions. We have addressed all the comments/suggestions in the revised manuscript. Detailed responses to the individual specific comment/suggestion are as follows.](#)

### **Major comments**

1. The PMF solution appears to be reasonable; however, I believe the authors need to do more to show that the PMF solution is robust. In Section 2.2, the authors state that comparisons were made to observations, emissions inventories, and previous PMF analyses, but no evidence is shown here or in the supplement to convince the reader

that this is true. Can the authors show the  $Q/Q_{\text{exp}}$  and explain why they settled on a 5-factor solution? What was the factor space used? Did the authors vary other parameters (e.g.  $F_{\text{peak}}$ ) or conduct a bootstrapping analysis to estimate uncertainty? Can the authors show the comparisons to other factor profiles reported in literature (e.g. the industrial factor compared to An et al., 2014).

I ask because PMF is partly subjective, and a more thorough discussion is necessary to justify why the authors settle on the solution presented in the manuscript. A 5-factor solution seems reasonable, and the factors discussed all appear to be consistent with the sources surrounding the sampling site, but this could be shown with more evidence in the main text or supplemental information.

Reply: The reviewer's valuable comment is highly appreciated. To provide more evidence for the selection of the five-factor solution from the PMF mode, the following text has been added in the revised manuscript:

*“The PMF model was tested using a variety of factor numbers, and the optimum source profiles and contributions were determined based on the correlation between modelled and observed data, the comparison of modelled profiles with the results from emission-based measurements, and previous studies involving PMF/other receptor model simulations (i.e., HKEPD, 2015; Wang et al., 2014; An et al., 2014; Liu et al., 2008a). For example, different solution with different factor numbers was explored and the source apportionment results from a five-factor resolution that could sufficiently explain the observed levels of VOCs were selected (details in Section 3.3). Compared with five-factor solution, the four-factor solution derived two profiles that attributable to gasoline and diesel vehicular exhaust, while most of the aromatic species in these sources and certain amounts of  $C_3$ - $C_4$  species from fuel evaporation were categorized under industrial emission. On the other hand, the six-factor solution has split a factor with high presence of ethyne and certain amounts of ethane (30% in species total),  $C_3$  species and benzene (~20% in species total), while some alkenes (18-80% in species total) were incorporated into fuel evaporation. Furthermore, the performance of the five-factor solution was evaluated using various checks and sensitivity tests. Suitable correlations between the observed concentrations and those of each species predicted*



by the model were observed, with the correlation coefficients ( $R^2$ ) ranging from 0.60 - 0.91, indicating that the solution adequately reproduced the observed variations of each species. All the scale residuals were within  $\pm 3\sigma$  with normal distributions for all species (Baudic et al., 2016). Moreover, different numbers of start seeds were tested during the simulation and no-multiple solutions were found. The ratio of  $Q(\text{robust})/Q(\text{true})$  obtained was  $\sim 0.93$ , close to 1 as suggested by previous studies and the user guide manual (Lau et al., 2010; Ling et al., 2016; Paatero, 2000). In addition, the results from bootstrapping analysis for the five-factor solution with bootstrap random seed found that all the factors were mapped to a basic factor in all the 20 bootstrap runs, while the uncertainties of each species from bootstrapping analysis were within the range of 1~20%. In this study, different  $F_{\text{peak}}$  values ranging from -5 to 5 was tested in the 5-factor solution for a more realistic profile (Lau et al., 2010; Baudic et al., 2016). The profiles with the nonzero  $F_{\text{peak}}$  values were consistent with those with zero  $F_{\text{peak}}$  value, reflecting that there was little rotation for the selected solution, confirming that the profiles were reasonably explained by the five-factor solution (Baudic et al., 2016). The results of  $F_{\text{peak}}$  value = 0.5 (the base run) was selected for analysis in this study. Overall, the above features demonstrated that the five-factor solution from PMF could provide reasonable and stable apportionment results for the observed VOCs at the JAES site.” For details, please refer to Lines 152-179, Pages 5-6 in the revised manuscript.

Furthermore, to justify the source apportionment results, more discussion based on the comparison of modelled profiles with the results from emission-based measurements, and other PMF model simulations were highlighted as follows:

“In this study, we applied the PMF model to apportion the sources of VOCs at the sampling site. Figure 4 illustrates the source profiles of the VOCs produced by the PMF model. Five VOC sources were resolved by PMF, including biogenic emissions (Source 1), fuel evaporation (Source 2), gasoline vehicular exhausts (Source 3), diesel vehicular exhausts (Source 4), and industrial emissions (Source 5).

Source 1 was identified as biogenic emissions due to the high loading of isoprene – a typical tracer of biogenic emissions (Yuan et al., 2012; Lau et al., 2010). Source 2 was represented by high proportions of 2-methylpentane, 3-methylpentane, i-pentane, and cyclopentane. Pentanes are mainly associated with profiles from gasoline-related emissions (Barletta et al., 2005; Tsai et al., 2006). However, the low contributions of incomplete combustion tracers in this profile suggested that the VOCs were sourced from fuel evaporation. The high presence of pentanes in this profile was consistent with the source profile of gasoline volatilization extracted from principal component analysis/absolute principal component scores (PCA/APCs) based on the observed VOC data collected in an industrial area of Nanjing (An et al., 2014), the source profile of gasoline evaporation from PMF at the suburban site and urban site in Beijing and Hong Kong (Yuan et al., 2009; Lau et al., 2010). Particularly, based on the emission-based measurement, Liu et al. (2008b) conducted source apportionments of VOCs in the Pearl River Delta region by the chemical mass balance (CMB) receptor model, which attributed the source with high loadings of n/i-pentanes, cyclopentane and 2/3-methylpentane as gasoline evaporation. Therefore, Source 2 here was identified as fuel evaporation.

Source 3 and Source 4 were identified as vehicular exhausts due to their high loadings of incomplete combustion tracers, i.e., C<sub>2</sub>-C<sub>4</sub> alkanes and alkenes (Zhang et al., 2018; Guo et al., 2011a, b). Zhang et al. (2018) compared the VOC composition of vehicular emissions from Zhujiang Tunnel in 2014 and 2004 in the Pearl River Delta region with those from other tunnel measurements. C<sub>2</sub>-C<sub>4</sub> alkanes and alkenes were found to make the greatest contributions to the loading of VOCs emitted from vehicles in 2014. The higher proportions of n/i-pentane, n-hexane, and methylcyclopentane in Source 3 relative to Source 4 indicated VOCs sourced from gasoline vehicular exhausts (Zhang et al., 2018; Guo et al., 2011b; Liu et al., 2008b). Source 4 was identified as diesel vehicular exhausts due to the high percentages of ethyne, ethane, and propene, as well as C<sub>2</sub>-C<sub>4</sub> alkenes (Ou et al., 2015; Liu et al., 2008c; Cai et al., 2010; Ho et al., 2009). Source 5 was characterized by high concentrations of aromatics. In addition to gasoline

vehicle emissions, industrial emission could be another important contributor to ambient aromatic hydrocarbons in the Yangtze River Delta, Pearl River Delta and North China Plain (Yuan et al., 2009; He et al., 2019; Zhang et al., 2013, 2014; Mo et al., 2015, 2017; An et al., 2014). The tunnel studies and emission-based measurement results found that aromatic hydrocarbons from gasoline vehicle exhaust were coherently emitted with pentanes, butenes, n-hexane, and cyclopentane, which were more consistent with the profile in source 3 mentioned above (Liu et al., 2008; Ho et al., 2009; Yuan et al., 2009; Zhang et al., 2018). Therefore, the absence of above species in source 5 indicated that this source could be related to industrial emission (Zhang et al., 2014). Particularly, the high presence of toluene, ethylbenzene, xylenes, ethyltoluene and trimethylbenzene was consistent with the emission-base measurement results conducted in paint and printing industries (Yuan et al., 2010) and manufacturing facilities (Zheng et al., 2013). On the other hand, the profile of high presence of aromatic hydrocarbons (C<sub>7</sub>-C<sub>9</sub> aromatics) and the certain amount of ethene, was also agree with the profiles measured in the areas dominated by industrial emissions in the Yangtze River Delta region (An et al., 2014; Shao et al., 2016; Mo et al., 2017). For example, An et al. (2014) reported that toluene, ethylbenzene, xylenes, and trimethylbenzenes could be emitted from different industrial processes, and identified that the factors with high loadings of these species as industrial production, solvent usage and industrial production volatilization sources by PAC/APCS at the industrial area in Nanjing. On the other hand, Mo et al. (2017) identified the factors with high concentrations of C<sub>7</sub>-C<sub>9</sub> aromatics and ethene as residential solvent usage, chemical and paint industries and petrochemical industry with the PMF model applied to the data collected in an industrialized coastal city of Yangtze River Delta region. To further identify source 3 and source 5, the ratio of toluene/benzene (T/B, ppbv/ppbv) in each profile was compared with those obtained from emission-based measurements and tunnel study results (Zhang et al., 2018 and references therein). The ratios of T/B were ~8.2 and ~1.2 for sources 5 and 3, respectively, and were consistent with those of “industrial processes and solvent application”, and “roadside and tunnel study”, respectively (Zhang et al., 2018 and references therein). This further confirmed that

*source 3 was related to gasoline vehicular exhaust, while source 5 was associated with industrial emission.”*

For details, please refer to Lines 388-440, Pages 13-15 in the revised manuscript.

## References:

- An, J.L., Zhu, B., Wang, H.L., Li, Y.Y., Lin, X., Yang, H., 2014. Characteristics and source apportionment of VOCs measured in an industrial area of Nanjing, Yangtze River Delta, China. *Atmospheric Environment* 97, 206-214.
- Barletta, B., Meinardi, S., Rowland, F.S., Chan, C.Y., Wang, X.M., Zou, S.C., Chan, L.Y., Blake, D.R., 2005. Volatile organic compounds in 43 Chinese cities. *Atmos. Environ.* 39 (32), 5979-5990.
- Baudic, A., Gros, V., Sauvage, S., Locoge, N., Olivier, S., Sarda-Esteve, R., Kalogridis, C., Petit, J.-E., Bonnaire, N., Baisnee, D., Favez, O., Albinet, A., Sciare, J., Bonsang, B., 2016. Seasonal variability and source apportionment of volatile organic compounds (VOCs) in the Paris megacity (France). *Atmospheric Chemistry and Physics* 16, 11961-11989.
- He, Z.R., Wang, X.M., Ling, Z.H., Zhao, J., Guo, H., Shao, M., Wang, Z., 2019. Contributions of different anthropogenic volatile organic compound sources to ozone formation at a receptor site in the Pearl River Delta region and its policy implication. *Atmospheric Chemistry and Physics* 19, 8801-8816.
- Ho, K.F., Lee, S.C., Ho, W.K., Blake, D.R., Cheng, Y., Li, Y.S., Ho, S.S.H., Fung, K., Louie, P.K.K., Park, D., 2009. Vehicular emission of volatile organic compounds (VOCs) from a tunnel study in Hong Kong. *Atmospheric Chemistry and Physics* 9, 7491-7504.
- Lau, A.K.H., Yuan, Z.B., Yu, J.Z., Louie, P.K.K., 2010. Source apportionment of ambient volatile organic compounds in Hong Kong. *Science of the Total Environment* 408, 4138-4149.
- Liu, Y., Shao, M., Lu, S.H., Chang, C.C., Wang, J.L., Fu, L.L., 2008. Source apportionment of ambient volatile organic compounds in the Pearl River Delta, China: Part II. *Atmospheric Environment* 42, 6261-6274.
- Mo, Z.W., Shao, M., Lu, S.H., Niu, H., Zhou, M.Y., Sun, J., 2017. Characterization of non-methane hydrocarbons and their sources in an industrialized coastal city, Yangtze River Delta, China. *Science of the Total Environment* 593-594, 641-653.
- Shao, P., An, J.L., Xin, J.Y., Wu, F.K., Wang, J.X., Ji, D.S., Wang, Y.S., 2016. Source apportionment of VOCs and the contribution to photochemical ozone formation during summer in the typical industrial area in the Yangtze River Delta, China. *Atmospheric Research* 176-177, 64-74.
- Tasi, W.Y., Chan, L.Y., Blake, D.R., Chu, K.W., 2006. Vehicular fuel composition and atmospheric emissions in South China: Hong Kong, Macau, Guangzhou, and Zhuhai. *Atmospheric Chemistry and Physics* 6, 3281-3288.
- Yuan, Z.B., Lau, A.K.H., Shao, M., Louie, P.K.K., Liu, S.C., Zhu, T., 2009. Source analysis of volatile organic compounds by positive matrix factorization in urban and rural environments in Beijing. *Journal of Geophysical Research* 114, D00G15, doi:10.1029/2008JD011190.
- Zhang, Y.L., Wang, X., Barletta, B., Simpson, I.J., Blake, D.R., Fu, X., Zhang, Z., He, Q., Liu, T., Zhao, X., Ding, X., 2013. Source attributions of hazardous aromatic hydrocarbons in urban, suburban and rural areas in the Pearl River Delta (PRD) region. *Journal of Hazardous Materials*

250, 403-411.

Zhang, Y.L., Yang, W.Q., Simpson, I.J., Huang, X.Y., Yu, J.Z., Huang, Z.H., Wang, Z.Y., Zhang, Z., Liu, D., Huang, Z.Z., Wang, Y.J., Pei, C.L., Shao, M., Blake, D.R., Zheng, J.Y., Huang, Z.J., 2018. Decadal changes in emissions of volatile organic compounds (VOCs) from on-road vehicles with intensified automobile pollution control: case study in a busy urban tunnel in south China. *Environmental Pollution* 233, 806-819.

Zheng, J.Y., Yu, Y.F., Mo, Z.W., Zhang, Z., Wang, X.M., Yin, S.S., Peng, K., Yang, Y., Feng, X.Q., Cai, H.H., 2013. Industrial sector-based volatile organic compound (VOC) source profiles measured in manufacturing facilities in the Pearl River Delta, China. *Science of the Total Environment* 456-457, 127-136.

2. The authors employ an OBM to evaluate ozone sensitivity to VOCs and NO<sub>x</sub>. OBMs are primarily useful because they allow one to evaluate relative incremental reactivity (as the authors describe in section 2.3). One strength of an OBM is that you do not need all of the measurements that described ozone formation; rather, you calculate source functions that explain residual effects on the time evolution of a measured species (e.g. meteorology, chemistry not accounted for in the mechanism, additional precursors that contribute to ozone formation, etc). From these calculations, you can derive the RIR by conducting a small perturbation on the system (e.g., decreasing or increasing the concentration of a species that is measured and well-represented by the model). The calculation of RIR are good and justified with the use of an OBM.

Reply: The reviewer's positive comment on OBM is highly appreciated. Yes, in this study, RIR which has been adopted in previous studies (i.e., Wang et al., 2017; Lyu et al., 2016; Xue et al., 2014; Cheng et al., 2010) as used to assess the sensitivity of precursors to photochemical O<sub>3</sub> formation by changing the concentrations of precursors (i.e., 10% reduction).

## References

Cheng, H.R., Guo, H., Wang, X.M., Saunders, S.M., Lam, S.H.M., Jiang, F., Wang, T., Ding, A., Lee, S., Ho, K.F., 2010. On the relationship between ozone and its precursors in the Pearl River Delta: application of an observation-based model (OBM). *Environmental Science and Pollution Research* 17, 547-560.

Lyu, X.P., Guo, H., Simpson, I.J., Meinardi, S., Louie, P.K.K., Ling, Z.H., Wang, Y., Liu, M., Luk, C.W.Y., Blake, D.R., 2016. Effectiveness of replacing catalytic converters in LPG-fueled vehicles in Hong Kong. *Atmospheric Chemistry and Physics* 16, 6609-6626.

Wang, Y., Wang, H., Guo, H., Lyu, X.P., Cheng, H.R., Ling, Z.H., Louie, P.K.K., Simpson, I.J.,

Meinardi, S., Blake, D.R., 2017. Long-term O<sub>3</sub>-precursor relationships in Hong Kong: field observation and model simulation. *Atmospheric Chemistry and Physics* 17, 10919-10935.

Xue, L.K., Wang, T., Gao, J., Ding, A.J., Zhou, X.H., Blake, D.R., Wang, X.F., Saunders, S.M., Fan, S.J., Zuo, H.C., Zhang, Q.Z., Wang, W.X., 2014. Ground-level ozone in four Chinese cities: precursors, regional transport and heterogeneous processes. *Atmospheric Chemistry and Physics* 14, 13175-13188.

In Section 3.4, the authors extend this analysis to evaluate the ozone isopleth. In this context, I don't believe the use of an OBM is justified. Isopleth calculation are defensible if a large fraction of the local, photochemically produced ozone is explained by the measured precursors. If a significant fraction of this produced ozone is explained by the time-dependent source function (i.e, the "residual" ozone), then the authors may not be measuring (or including in the model) a significant fraction of the VOC precursors needed to derive ozone formation. In that case, how can the authors determine whether Nanjing is VOC or NO<sub>x</sub>-sensitive? The isopleth presented in Fig.6 is very NO<sub>x</sub> saturated, which the authors say generally agrees with previous literature. But do the measurements really defend this?

Reply: Thanks a lot for the reviewer's comment. We agree with the reviewer that the isopleth calculation could be reasonable when photochemically produced ozone from the measured precursors made a significant contribution to observed O<sub>3</sub>. As the O<sub>3</sub> simulated by the OBM was derived based on the observed mixing ratios of precursors and local meteorology, it is more appropriate to refer the simulation of O<sub>3</sub> by the OBM as local produced O<sub>3</sub>, though the observed mixing ratios of precursors could be both influenced by local emissions and those transported from upwind areas (Liu et al., 2019). Therefore, before using the isopleth calculation, it is necessary to investigate whether locally produced O<sub>3</sub> from OBM could make a significant portion to the observed O<sub>3</sub> at the JAES site. The investigation on the wind parameters found that the average wind speed was ~1.8 m/s on O<sub>3</sub> episode days, with about ~51% of most wind speed data being ≤ 2 m/s (see Figure S2 in the supplementary), suggesting that regional transport may not have a significant influence on the levels of O<sub>3</sub> and its precursors on episode days at the JAES site (Shao et al., 2016; Wang et al., 2017).

Figure S3 in the supplementary showed the timeseries for the comparison between local

produced O<sub>3</sub> from OBM and the observed O<sub>3</sub> mixing ratios, while Figure S4 in the supplementary presented the comparison between the mean diurnal variations of simulated and observed O<sub>3</sub> mixing ratios for all the O<sub>3</sub> episode days at the JAES site. It was found that the model underestimated or overestimated O<sub>3</sub> on some episode days. The comparison between the mean diurnal variations of simulated and observed O<sub>3</sub> suggested that the model captured the diurnal variations of O<sub>3</sub>, and the predicted and observed maximum O<sub>3</sub> values were comparable, though the predicted mixing ratios of O<sub>3</sub> were lower than that observed in the early morning. The above discrepancy between observed and predicted O<sub>3</sub> mixing ratios was mainly due to the failure to consider physical processes (i.e., horizontal and vertical transport) and/or the other O<sub>3</sub> precursors (i.e., carbonyls and other oxygenated VOCs (OVOCs)) (Liu et al., 2019; Cheng et al., 2010; Shao et al., 2009a). However, the simulation indeed provided a reasonable description of the O<sub>3</sub> variations using the observation data. To assess the local photochemically produced O<sub>3</sub> against the measured levels of O<sub>3</sub> during the O<sub>3</sub> episode days, the amount of the locally produced O<sub>3</sub> formed by the photochemistry was compared with the observed O<sub>3</sub> accumulations that were calculated as difference between the peak and early-morning concentrations of O<sub>3</sub>. The amount of local photochemically produced O<sub>3</sub> was determined by the net O<sub>3</sub> production rate, which was calculated by the difference between the gross production G(O<sub>3</sub>) and destruction rates D(O<sub>3</sub>) in the model (Equations 1-3).

$$P(O_3) = G(O_3) - D(O_3) \quad (1)$$

$$G(O_3) = k_{HO_2+NO}[HO_2][NO] + \sum k_{RO_2i+NO}[RO_{2i}][NO] \quad (2)$$

$$D(O_3) = k_{HO_2+O_3}[HO_2][O_3] + k_{OH+O_3}[OH][O_3] + k_{O(^1D)+H_2O}[O(^1D)][H_2O] + k_{OH+NO_2}[OH][NO_2] + k_{alkenes+O_3}[alkenes][O_3] \quad (3)$$

Where the  $k$  constant values were the rate coefficients for the subscript reaction. The detailed description for the above calculation was provided by Xue et al. (2013, 2014) and Wang et al. (2017). At JAES, the daytime (07:00–19:00 LT) average net O<sub>3</sub> production rate was estimated to be 6.2 ppbv h<sup>-1</sup>, corresponding to ~74 ppbv O<sub>3</sub> formed from local photochemistry during daytime hours. The amount was coincident with the average increment of O<sub>3</sub> observed from early morning to late afternoon at JAES (~81

ppbv), suggesting that local photochemically produced O<sub>3</sub> significantly contributed to the O<sub>3</sub> increment at JAES. Indeed, the observed minimum O<sub>3</sub> mixing ratios before accumulation which were considered as the residual O<sub>3</sub> levels (or background O<sub>3</sub>, the mean value was 20 ppbv) at the sampling site as suggested by the previous studies (Xue et al., 2013, 2014a,b) only accounted for ~20% of the observed maximum O<sub>3</sub> values (the mean value was 102 ppbv) (data not shown). Furthermore, the difference between observed and simulated minimum O<sub>3</sub> mixing ratios which was considered as the fraction of residual O<sub>3</sub> that could not be explained by the OBM model only contributed ~17% of the observed maximum O<sub>3</sub> mixing ratio. The above analysis on the difference between observed and simulated O<sub>3</sub> levels confirmed that local photochemical produced O<sub>3</sub> made a significant fraction to observed O<sub>3</sub> levels at JAES. However, we admitted that the OBM model could not accurately estimate the contributions of residual O<sub>3</sub> to the increment of O<sub>3</sub> values during daytime, which requires to be studied using a combination of different models and dataset (i.e., the regional air quality model, Lagrangian dispersion model and emission inventory) (Wang et al., 2015; Ding et al., 2013a, b; Jiang et al., 2010).

To further evaluate the model performance, the index of agreement (IOA) that was developed to assess the agreement between modelled and observed results was used in this study (Huang et al., 2005; Wang et al., 2013, 2015; Liu et al., 2019). The calculation of IOA was as follows:

$$IOA = 1 - \frac{\sum_{i=1}^n (O_i - S_i)^2}{\sum_{i=1}^n (|O_i - \bar{O}| + |S_i - \bar{O}|)^2} \quad (4)$$

Where  $S_i$  and  $O_i$  were the simulated and observed O<sub>3</sub>, respectively, while  $\bar{O}$  was the mean of observed O<sub>3</sub>, and  $n$  is the number of samples. The IOA values ranged between 0 and 1, and a relatively higher value of IOA indicated relatively greater consistency between simulated results and observation data (Wang et al., 2013, 2015, 2017). In this study, the IOA of O<sub>3</sub> was ~0.85, suggesting consistency of the abundance and variation



of O<sub>3</sub> between the observation and simulation, and demonstrating that locally produced O<sub>3</sub> could be explained by the measured precursors.

In the atmosphere, the sensitivity of photochemical O<sub>3</sub> formation was distributed into three regimes, including the VOC-limited regime, the NO<sub>x</sub>-limited regime and the transitional regime. In the VOCs-limited regime (the relative concentration [NO<sub>x</sub>]/[VOC] is high and/or NO<sub>x</sub> is saturated), photochemical O<sub>3</sub> formation decreases with the decrease in the concentration of VOCs (resulting from the control of VOC emissions), while in the NO<sub>x</sub>-limited regime (high [VOC]/[NO<sub>x</sub>] ratio and/or VOC is saturated), any reduction in the NO<sub>x</sub> concentration would shorten the O<sub>3</sub> formation chain length and reduces the photochemical O<sub>3</sub> formation (Jenkin and Clemitshaw, 2000). The mean mixing ratios of NO<sub>x</sub> and TVOCs during daytime hours (0700-1800 LT, local time) on O<sub>3</sub> episode days were  $19.2 \pm 1.2$  ppbv, respectively, with the mean ratio of VOCs/NO<sub>x</sub> as (ppbC/ppbv)  $\sim 3.4$ , suggested that the atmosphere in at the JAES site was NO<sub>x</sub> saturated and photochemical O<sub>3</sub> formation located in the VOC-regime (Jenkin and Clemitshaw, 2000). However, it should be noted that using the ratios of VOCs/NO<sub>x</sub> to determine the O<sub>3</sub> formation regime could be biased in different environments as different VOC species react at different rates and with different reaction mechanisms, thus inducing the nonlinear dependency of O<sub>3</sub> formation on NO<sub>x</sub> and VOCs. Figure 6 shows the O<sub>3</sub> isopleth plot illustrating the relationship between VOCs and NO<sub>x</sub> concentrations on the O<sub>3</sub> mixing ratio. The plot is the output from the OBM-MCM model, and is based on the mean diurnal variability of observed air pollutants on O<sub>3</sub> episode days. Based on the current scenario (with 100% of observed mixing ratios of VOCs and NO<sub>x</sub>, point A in Figure 6), the O<sub>3</sub> mixing ratio decreased with the reduction of VOCs and increased with the reduction of NO<sub>x</sub>, indicating that O<sub>3</sub> formation in this site is VOC-limited. Furthermore, to accurately evaluate the O<sub>3</sub>-precursor relationship, the RIR values from the OBM model, which were frequently used to evaluate the O<sub>3</sub> formation sensitivity based on observation data, were further explored. Positive RIR values were found for the VOCs (see Figure 7a), while negative values were found for NO<sub>x</sub> (i.e.,  $-0.25 \pm 0.02$ ), further confirming that O<sub>3</sub> formation at

the JAES site was VOC-limited (Zhang et al., 2008; Shao et al., 2009b; Cheng et al., 2010).

Overall, the above analysis confirmed that simulation of OBM could be used to conduct O<sub>3</sub> isopleth calculation and investigate the O<sub>3</sub>-precursor relationship (Shao et al., 2016; Lyu et al., 2019; He et al., 2019).

The above evaluation on the OBM model performance has been provided in Lines 209-266, Pages 7-9 in the revised manuscript, while the O<sub>3</sub>-precursor relationship evaluated by the observed data, O<sub>3</sub> isopleth plot and RIR values from the OBM-MCM model was provided in details in Lines 511-533, Page 18 in the revised manuscript.

## References

- Cheng, H.R., Guo, H., Wang, X.M., Saunders, S.M., Lam, S.H.M., Jiang, F., Wang, T., Ding, A., Lee, S., Ho, K.F., 2010. On the relationship between ozone and its precursors in the Pearl River Delta: application of an observation-based model (OBM). *Environmental Science and Pollution Research* 17, 547-560.
- Ding, A.J., Fu, C.B., Yang, X.Q., Sun, J.N., Zheng, L.F., Xie, Y.N., Herrmann, E., Nie, W., Petäjä, T., Kerminen, V.-M., Kulmala, M., 2013a. Ozone and fine particle in the western Yangtze River Delta, an overview of 1 yr data at the SORPES station. *Atmospheric Chemistry and Physics* 13, 5813-5830.
- Ding, A.J., Wang, T., Fu, C.B., 2013b. Transport characteristics and origins of carbon monoxide and ozone in Hong Kong, South China. *Journal of Geophysical Research* 118, doi: 10.1002/jgrd.50714.
- Huang, J.P., Fung, J.C.H., Lau, A.K.H., Qin, Y., 2005. Numerical simulation and process analysis of typhoon-related ozone episodes in Hong Kong. *Journal of Geophysical Research* 110, D05301, doi:10.1029/2004JD004914.
- Jenkin, M.E. and Clemitshaw, K.C., 2000. Ozone and other secondary photochemical pollutants: chemical processes governing their formation in the planetary boundary layer. *Atmospheric Environment* 34, 2499-2527.
- Jiang, F., Guo, H., Wang, T.J., Cheng, H.R., Wang, X.M., Simpson, I.J., Ding, A.J., Saunders, S.M., Lam, S.H.M., Blake, D.R., 2010. An ozone episode in the Pearl River Delta: field observation and model simulation. *Journal of Geophysical Research* 115, D22, doi: 10.1029/2009JD013593.
- Liu, X., Lyu, X., Wang, Y., Jiang, F., Guo, H., 2019. Intercomparison of O<sub>3</sub> formation and radical chemistry in the past decade at a suburban site in Hong Kong. *Atmospheric Chemistry and Physics* 19, 5127-5145.
- Lyu, X.P., Wang, N., Guo, H., Xue, L.K., Jiang, F., Zeren, Y.Z., Cheng, H.R., Cai, Z., Han, L.H., Zhou, Y., 2019. Causes of a continuous summertime O<sub>3</sub> pollution event in Jinan, a central city

- in the North China Plain. *Atmospheric Chemistry and Physics* 19, 3025-3042.
- Shao, M., Zhang, Y.H., Zeng, L.M., Tang, X.Y., Zhang, J., Zhong, L.J., Wang, B.G., 2009b. Ground-level ozone in the Pearl River Delta and the roles of VOC and NO<sub>x</sub> in its production. *Journal of Environmental Management* 90, 512-518.
- Shao, P., An, J.L., Xin, J.Y., Wu, F.K., Wang, J.X., Ji, D.S., Wang, Y.S., 2016. Source apportionment of VOCs and the contribution to photochemical ozone formation during summer in the typical industrial area in the Yangtze River Delta, China. *Atmospheric Research* 176-177, 64-74.
- Wang, N., Guo, H., Jiang, F., Ling, Z.H., Wang, T., 2015. Simulation of ozone formation at different elevations in mountainous area of Hong Kong using WRF-CMAQ model. *Science of the Total Environment* 505, 939-951.
- Wang, N., Guo, H., Jiang, F., Ling, Z.H., Wang, T., 2015. Simulation of ozone formation at different elevations in mountainous area of Hong Kong using WRF-CMAQ model. *Science of the Total Environment* 505, 939-951.
- Wang, N., Guo, H., Jiang, F., Ling, Z.H., Wang, T., 2015. Simulation of ozone formation at different elevations in mountainous area of Hong Kong using WRF-CMAQ model. *Science of the Total Environment* 505, 939-951.
- Wang, X.M., Liu, H., Pang, J.M., Carmichael, G., He, K.B., Fan, Q., Zhong, L.J., Wu, Z.Y., Zhang, J.P., 2013. Reductions in sulfur pollution in the Pearl River Delta region, China: assessing the effectiveness of emission controls. *Atmospheric Environment* 76, 113-124.
- Wang, Y., Wang, H., Guo, H., Lyu, X.P., Cheng, H.R., Ling, Z.H., Louie, P.K.K., Simpson, I.J., Meinardi, S., Blake, D.R., 2017. Long-term O<sub>3</sub>-precursor relationships in Hong Kong: field observation and model simulation. *Atmospheric Chemistry and Physics* 17, 10919-10935.
- Xue, L.K., Wang, T., Guo, H., Blake, D.R., Tang, J., Zhang, X.C., Saunders, S.M., Wang, W.X., 2013. Sources and photochemistry of volatile organic compounds in the remote atmosphere of western China: results from the Mt. Waliguan Observatory. *Atmospheric Chemistry and Physics* 13, 8551-8567.
- Xue, L.K., Wang, T., Wang, X.F., Blake, D.R., Gao, J., Nie, W., Gao, R., Gao, X.M., Xu, Z., Ding, A.J., et al., 2014. On the use of an explicit chemical mechanism to dissect peroxy acetyl nitrate formation. *Environmental Pollution* 195, 39-47.
- Zhang, Y.H., Su, H., Zhong, L.J., Cheng, Y.F., Zeng, L.M., Wang, X.S., Xiang, Y.R., Wang, J.L., Gao, D.F., Shao, M., Fan, S.J., Liu, S.C., 2008. Regional ozone pollution and observation-based approach for analyzing ozone-precursor relationship during the PRIDE-PRD2004 campaign. *Atmospheric Environment* 42, 6203-6218.

If the authors are to present an ozone isopleth, then I believe there needs to be a much larger discussion describing how well the OBM performs in reproducing observed ozone mixing ratios. Without much discussion, I can only assume that there is residual ozone that is explained by the time-dependent source functions derived through OBM calculations, and not by the precursors measured by the precursors measured by GC. How much of the ozone calculated via OBM is explained by the precursors measured by the GC, and how much of the ozone is unexplained? Can the authors show an

analysis (perhaps just a time series) showing ozone explained by the precursors, and ozone explained by the source function? This helps place into context the extent to which the measured VOCs were the primary contributors to ozone observed at the ground site.

Reply: Thanks for the reviewer's comment. Figure S3 and Figure S4 in the supplementary presented the comparisons between the simulated and observed O<sub>3</sub> during O<sub>3</sub> episode days at the JAES site. From the reply of the above comment, it could be concluded that the simulation of OBM could reproduce the observed variations of O<sub>3</sub> during O<sub>3</sub> episode days at the JAES site and the measured VOCs indeed explained the major fraction of observed O<sub>3</sub> levels, with the IOA index of 0.85 between simulation and observation results. The amount of the unexplained O<sub>3</sub> which could be related to the time-dependent source (*i.e.*, the residual O<sub>3</sub>) was estimated roughly to be ~17%. However, we agreed with the reviewer that the OBM model could not accurately estimate the contributions of residual O<sub>3</sub> to the increment of O<sub>3</sub> values during daytime, which requires to be studies using a combination of different models and dataset (*i.e.*, the regional air quality model, Lagrangian dispersion model and emission inventory) (Wang et al., 2015; Ding et al., 2013a, b; Jiang et al., 2010).

The detailed discussion on the performance of model simulation on O<sub>3</sub> formation has been provided in Lines 209-266, Pages 7-9 in the revised manuscript.

Finally, the authors also need to provide more details about the OBM itself. The only description of how the model was tailored the Nanjing observations is provided at lines 135-140. What meteorological conditions were used? If this observation-based, I assume that dilution by PBL expansion and wind speed are lumped into the source functions, but what about incident solar radiation? How do the authors calculate photolysis frequencies? Did the authors use a model, such as TUV, or was there a solar spectrum measurement? Can the author provide a JNO<sub>2</sub> frequency to orient the readers? The authors constrain CO, NO<sub>x</sub>, SO<sub>2</sub>, and O<sub>3</sub>. How were these species measured, what instrumentation, and how was this instrumentation calibrated? Finally, when were the O<sub>3</sub> episodes? A time series showing ozone over the course of the campaign would be useful?

Reply: Thanks for the reviewer's comment. In this study, the meteorological conditions, including the temperature, relative humidity and pressure were incorporated into the model. These parameters, together with wind speed and direction were monitored by a weather station (Vantage Pro TM & Vantage Pro 2 plus TM Weather Stations, Davis Instruments). In the model, the height of the boundary layer was configured to increase gradually from ~300 m in the morning to ~1500 m in the afternoon and then collapsed back to 300 m at night based on the radiosonde and reanalysis data in China (Guo et al., 2016). On the other hand, as neither the photolysis of O<sub>3</sub> (J(O<sup>1</sup>D)) nor that of NO<sub>2</sub> (J(NO<sub>2</sub>)) was measured in this study, the photolysis frequencies, including j(O<sup>1</sup>D), j(NO<sub>2</sub>) and photolysis rates of other species were calculated using the photon flux determined from the Tropospheric Ultraviolet and Visible Radiation model (TUV, version 5.3, [http://cprm.acom.ucar.edu/Models/TUV/Interactive\\_TUV/](http://cprm.acom.ucar.edu/Models/TUV/Interactive_TUV/), access date: 03 Jan 2020) based on the actual conditions, such as solar radiation, location and time period of the field campaign in Nanjing. The parameterization for the scheme of the TUV (v5.3) module can be found in the code of MCM (<http://mcm.leeds.ac.uk/MCMv3.3.1/home.htm>, access date: 07 Jan 2010). Additional information on the model calculation and performance has been reported in the previous studies (Pinho et al., 2009; Lam et al., 2013; Shao et al., 2016; Wang et al., 2017). Figure S1 in the supplementary presented the mean diurnal pattern of J(NO<sub>2</sub>) simulated by the OBM model using TUV scheme. A typical solar-driven diurnal cycle with the maximum value ( $\sim 11.1 \times 10^{-3} \text{ s}^{-1}$ ) at noon (1100-1200 LT) were observed in the photolysis of J(NO<sub>2</sub>), which was consistent with those observed and modelled in China (Wang et al., 2019; Li et al., 2011), suggesting that the simulated photolysis frequencies using the TUV scheme in the model was appropriate in the present study.

The incorporation of meteorological conditions into the OBM-MCM model, the configuration of planetary boundary layer and the calculation of photolysis frequencies of different species have been provided as above in the revised manuscript. For details, please refer to Lines 190-205, Pages 6-7 in the revised manuscript.

Furthermore, the information for the measurement of trace gases, including O<sub>3</sub>, NO<sub>x</sub>,

CO and SO<sub>2</sub> was provided as follows:

*“On the other hand, trace gases including CO, NO-NO<sub>2</sub>-NO<sub>x</sub>, SO<sub>2</sub>, and O<sub>3</sub> were measured at 1-min resolution using the commercial instruments of TEI 48i, 42i, 43i and 49i (Thermo Electron Corporation). All these instruments were zero checked daily, span calibrated weekly and multi-point calibrated monthly. Furthermore, meteorological conditions, including the temperature, relative humidity, pressure, wind speed and direction were monitored at 1-min resolution by a weather station (Vantage Pro TM & Vantage Pro 2 plus TM Weather Stations, Davis Instruments).”*

For details, please refer to Lines 133-138, Page 5 in the revised manuscript.

On the other hand, according to the comment, Figure S7 in the supplementary presented the time series of air pollutants for the whole sampling period. In this study, total 88 O<sub>3</sub> episode days (identified as hourly maximum O<sub>3</sub> concentrations > 80 ppbv per day) were selected for further analysis.

#### Reference

- Guo, J.P., Miao, Y.C., Zhang, Y., Liu, H., Li, Z.Q., Zhang, W.C., He, J., Lou, M.Y., Yan, Y., Bian, L.G., Zhai, P.M., 2016. The climatology of planetary boundary layer height in China derived from radiosonde and reanalysis data. *Atmospheric Chemistry and Physics* 16, 13309-13319.
- Lam, S.H.M., Saunders, S.M., Guo, H., Ling, Z.H., Jiang, F., Wang, X.M., Wang, T.J., 2013. Modelling VOC source impacts on high ozone episode days observed at a mountain summit in Hong Kong under the influence of mountain-valley breezes. *Atmospheric Environment* 81, 166-176.
- Li, J., Wang, Z.F., Wang, X., Yamaji, K., Takigawa, M., Kanaya, Y., Pochanart, P., Liu, Y., Irie, H., Hu, B., Tanimoto, H., Akimoto, H., 2011. Impacts of aerosols on summertime tropospheric photolysis frequencies and photochemistry over Central Eastern China. *Atmospheric Environment* 45, 1817-1829.
- Pinho, P.G., Lemos, L.T., Pio, C.A., Evtuyugina, M.G., Nunes, T.V., Jenkin, M.E., 2009. Detailed chemical analysis of region-scale air pollution in western Portugal using an adapted version of MCM v3.1. *Science of the Total Environment* 407, 2024-2038.
- Shao, P., An, J.L., Xin, J.Y., Wu, F.K., Wang, J.X., Ji, D.S., Wang, Y.S., 2016. Source apportionment of VOCs and the contribution to photochemical ozone formation during summer in the typical industrial area in the Yangtze River Delta, China. *Atmospheric Research* 176-177, 64-74.
- Wang, W.J., Li, X., Shao, M., Hu, M., Zeng, L.M., Wu, Y.S., Tan, T.Y., 2019. The impact of aerosols on photolysis frequencies and ozone production in Beijing during the 4-year period 2012-2015. *Atmospheric Chemistry and Physics* 19, 9413-9429.
- Wang, Y., Wang, H., Guo, H., Lyu, X.P., Cheng, H.R., Ling, Z.H., Louie, P.K.K., Simpson, I.J.,

Meinardi, S., Blake, D.R., 2017. Long-term O<sub>3</sub>-precursor relationships in Hong Kong: field observation and model simulation. *Atmospheric Chemistry and Physics* 17, 10919-10935.

### **Other comments**

Line 112: PMF can be conducted using many tools. Is this the US EPA model, SoFi, another model, or one that was developed by Yuan et al. or Ling et al.? This should be noted here, with a relevant reference if necessary.

Reply: Thanks for pointing this out. The US EPA PMF model was used in this study.

To verify it, the sentence has been revised as follows:

*“In this study, the US EPA PMF (version 4.1) model, which has been widely used to conduct source apportionment of VOCs (He et al., 2019 and references therein; Mo et al., 2017; Zhang et al., 2013), was applied to the observed VOC data to identify potential VOC sources.”*

For details, please refer to Line 140, Page 5 in the revised manuscript.

Line 120: Shao et al. discuss VOC reactivity through analysis of maximum incremental reactivity (MIR) and by calculating propylene-equivalent concentration. Which method are you referring to?

Reply: Thanks for pointing this out. To clarify the method used to investigate total reactivity of NMHCs, the following sentence has been revised as follows:

*“..... of the total measured VOCs through the analysis of maximum incremental reactivity (MIR) (Shao et al., 2009a).”*

For details, please refer to Lines 149-150, Page 5 in the revised manuscript.

Line 130: please provide references for the MCM (see the following website for appropriate references depending on the sub mechanisms used: <http://mcm.leeds.ac.uk/MCMv3.2/citation.htm>).

Reply: Thanks for the reviewer's comment. References for MCM mechanism have been added as follows:

*“In this study, we applied the observation-based model (OBM) coupled with the MCM (version 3.2) (<http://mcm.leeds.ac.uk/MCMv3.2/citation.htm>, Lyu et al., 2016; Ho et al.,*

2019)...”

For details, please refer to Lines 181-182, Page 6 in the revised manuscript.

Also, is there a reason that v 3.2 was used, rather than 3.3.1? v3.3.1 has updates to the isoprene mechanism that may (or may not) be relevant here.

Reply: Thank for the reviewer’s comment. Compared with version 3.2, MCM version 3.3.1 have the following updates: 1) The updates of HO<sub>x</sub> recycling which has a collectively significant impact on OH radical regeneration at lower NO<sub>x</sub> levels. 2) The updates of NO<sub>x</sub> recycling which include the formation of species that have been reported to play a role in SOA-formation mechanisms, including epoxydiols (initially implemented in MCM v3.2), hydroxymethyl-methyl- $\alpha$ -lactone (HMML) and methacrylic acid epoxide (MAE). These above updates may not be relevant to the present study as the levels of NO<sub>x</sub> at the JAES site were not low, with the average mixing ratios of  $25 \pm 1$  (mean  $\pm$  95% confidence interval) ppbv in 2016. Furthermore, the present study only focused on the roles of VOCs on O<sub>3</sub> formation through gas-phase mechanisms which may not be influenced by the NO<sub>x</sub> recycling updates for SOA formation. However, we did try our best to incorporate the version 3.3.1 MCM into our photochemical box model to evaluate the roles of NMHCs on SOA formation, which is still under construction (Ling et al., “Formation and sink of glyoxal and methylglyoxal in a polluted subtropical environment: observation-based photochemical analysis and impact evaluation”, unpublished manuscript).

Line 164: By TVOC, you mean the sum of measured VOCs?

Reply: Yes. It has been revised as follows:

*“The annual average total VOC (TVOC, sum of the measured VOCs)...”*

For details, please refer to Line 292, Page 9 in the revised manuscript.

Line 172: Is this reversed? The first number (referring to weekdays) is lower than the second (referring to weekends).

Reply: Sorry for the mistake. It has been revised accordingly. For details, please refer



to Lines 299-300, Page 10 in the revised manuscript.

Table 1: You only give an average and standard deviation - no mixing ratio ranges are shown. I recommend removing "range".

Reply: Thanks for the reviewer's comment. The "range" has been removed accordingly. For details, please refer to Table 1 in the revised manuscript.

Line 194: Continuous VOC measurements have been available much longer than this in other countries. I would recommend changing this wording to say "online VOC measurements have been available for multiple decades"

Reply: Thanks for the suggestion. The sentence has been revised as "...online VOC measurements have been available for multiple decades..."

For details, please refer to Lines 320-321, Page 11 in the revised manuscript.

Fig.2 This is a nice benchmark of the Nanjing measurements with other cities during a period when developed countries were still reducing mobile emissions (mid 1990s – early 2000s). How does this compare with measurements conducted in developed countries today? It would be nice to see how the mixture in Nanjing compared to London or Los Angeles today, and would also highlight the gap that could be achieved with further VOC reductions.

Reply: Thanks a lot for the reviewer's positive comment. In this study, to highlight the variations of VOCs in different regions, comparison of annual average concentrations of ambient VOCs in different cities based on real-time online continuous measurements of at least one year was present in Figure 2. We do try our best to find as many studies focusing on the long-term (at least one-year) variations of VOCs in developed regions/countries as possible. The results presented in Figure 2 were all the data we can get. It was found that the current ambient VOC concentrations in Chinese megacities are generally comparable to the urban VOC levels in developed countries during the year 2000. However, in developed countries, the mixing ratios of VOCs were observed to decrease in the recent decades following the implementation and formulation of VOC

strategies (Warneke et al., 2012). For example, the mixing ratios of VOCs in Los Angeles have decreased significantly from 1960-2002 at an average annual rate of ~7.5%, while the mixing ratios of VOCs in London presented a higher and faster decrease since 1998 when there were higher VOC mixing ratios than those in Los Angeles, confirming that the earlier implementation of VOC reduction strategies in California had clearly led to the earlier improvement of air quality compared to London (Warneke et al., 2012; von Schneidemesser et al., 2010). Chinese megacities are therefore experiencing significantly higher ambient VOCs contamination, given the remarkable decrease in VOC emissions in developed countries over the last two decades (European Environment Agency, 2016; U.S. EPA, 2017; Pan et al., 2015). High VOC levels in Chinese megacities are known to impact ambient ozone and secondary particle pollution, as well as cause adverse impacts on human health. However, as China has a solid foundation for VOCs monitoring and control, numerous strict, appropriate and targeted reduction strategies for VOCs have been/are being formulated and implemented in Chinese megacities (Guo et al., 2017). It is expected these measures could help China to reduce VOC emissions/mixing ratios and improve air quality in the future.

To highlight the reduction of VOCs in developed regions and the gap that could be achieved with further VOC reductions in China, the above discussion has been added in the revised manuscript. For details, please refer to Lines 333-347, Pages 11-12 in the revised manuscript.

## Reference

- Guo, H., Ling, Z.H., Cheng, H.R., Simpson, I.J., Lyu, X.P., Wang, X.M., Shao, M., Lu, H.X., Ayoko, G., Zhang, Y.L., Saunders, S.M., Lam, S.H.M., Wang, J.L., Blake, D.R., 2017. Science of the Total Environment 574, 1021-1043.
- von Schneidemesser, E., Monks, P.S., Plass-Duelmer, C., 2010. Global comparison of VOC and CO observations in urban areas. Atmospheric Environment 44, 5053-5064.
- Warneke, C., de Gouw, J.A., Holloway, J.S., Peischl, J., Ryerson, T.B., Atlas, E., Blake, D., Trainer, M., Parrish, D.D., 2012. Multiyear trends in volatile organic compounds in Los Angeles, California: Five decades of decreasing emissions. Journal of Geophysical Research 117, D00V17, doi: 10.1029/2012JD017899.

Lines 227-228: Can the authors briefly summarize the conclusions from Wang et al., 2013? Was it due to changes in prevailing winds, or simply due to build up of pollutants during strong inversions?

Reply: Thanks for the reviewer's comment. In Shanghai, relative high levels of VOCs were observed from October to January of the following year and from June to July based on the two-year measurement conducted from 2009 to 2010 (Wang et al., 2013). The inversion layer, the effect of cold front or uniform pressure in winter resulted in high levels of VOCs from October to January of the following year, while the frontal inverted trough or frequently observed stagnant high pressure system with southwest flow that could lead to poor diffusion were unfavorable meteorological conditions for high VOC levels from June to July. In addition, air masses transported from upwind chemical and petrochemical industrial factories located in the southwest and south of the monitoring site was another factor for the high VOC levels in summer (*i.e.*, June and July) and winter.

The above brief summary for the monthly variations of VOC levels in Shanghai have been provided in the revised manuscript. For details, please refer to Lines 363-370, Pages 12-13 in the revised manuscript.

Line 280-281: As the authors note, these differences result, in part, due to the proximity of the different sampling campaigns. However, I think it's also good to note why these differences are important. How much of the population resides in the sampled region? Is the mix measured in a more residential area more important for human exposure? This is certainly a nice motivation to look at the spatial VOC distributions in Nanjing in the future.

Reply: Thanks for the comment. The sampling site (*i.e.*, the JAES site) was located at a more residential and urban area compared to other sites listed in An et al. (2014) and Xia et al. (2014). There are more than 0.22 million people living in the areas surrounding the sampled site (within 3 km of the observation site) which composed of residential communities, schools, government agencies, and business centers.

The above description on the sampling surrounding was added in the Lines 456- 460,

Page 16 in the revised manuscript.

Line 319: Do you mean that you averaged the PMF solutions during the ozone episodes and non-episode days to look at differences?

Reply: Yes. To make it clearer, we have revised as follows:

*“... we extracted and averaged the contributions of the different sources on these O<sub>3</sub> episode days from the PMF model...”*

For details, please refer to Lines 509-510, Page 17 in the revised manuscript.

Figure 6. The isopleth description is somewhat confusing-is this % change in NO<sub>x</sub> and VOCs, or % of base-case VOCs.

Reply: Sorry for the mistake and confusion it caused. The horizontal and vertical axes in Figure 6 correspond to the percentage of base-case VOCs and NO<sub>x</sub>. It has been revised accordingly in the caption of Figure 6.

Section 3.5. Without more work to convince the reader that the ozone isopleth is reasonable, I believe these statements would need to be amended. First, the authors haven't shown that the ozone precursors measured account for the majority of the ozone modeled in the OBM. Second, the recommendation to prioritize VOC reductions (line 381) is very likely to matter on a local level (as alluded to by the authors), but what about ozone formation on regional scales? In other countries, downwind of major cities, ozone formation transitions to NO<sub>x</sub>-sensitive due to the abundance of biogenic sources that can react alongside NO<sub>x</sub> (e.g. Trainer et al., 1987). I think this should be discussed as well, since NO<sub>x</sub> reductions matter and are important in the long run.

Reply: We highly appreciated for the reviewer's comment. As discussed previously, the simulation of OBM model could reproduce the observed variations of O<sub>3</sub> and the measured O<sub>3</sub> precursor indeed contributed a major fraction for the model O<sub>3</sub> from OBM and the observed O<sub>3</sub> mixing ratios. On the other hand, we agreed with the reviewer that the results in the present study were based on the local measurement conducted at the urban site of Nanjing city, which likely presented a local perspective. The

recommendation to prioritize VOC reductions was likely matter to the urban area where O<sub>3</sub> formation was VOC-limited. However, O<sub>3</sub> pollution is a regional cross-boundary environmental issue rather than a local pollution problem. Apart from VOCs, NO<sub>x</sub> was another important precursor for O<sub>3</sub> formation with its dual roles in O<sub>3</sub> production (enhancing O<sub>3</sub> formation in non NO<sub>x</sub>-saturated environment and titrating O<sub>3</sub> in NO<sub>x</sub>-saturated environment). In other areas (i.e., the rural environment and/or the downwind areas of urban center in the same region) where the concentrations of NO<sub>x</sub> are low and/or there is a non NO<sub>x</sub>-saturated environment, the situation may be different and controlling VOCs should be conducted cautiously (Ou, et al., 2016; Yuan et al., 2013; Zheng et al., 2010). Therefore, from a regional perspective, the benefits of VOCs control measures could be further evaluated with those of NO<sub>x</sub> (i.e., the appropriate ratios of VOC/NO<sub>x</sub> for the reduction of O<sub>3</sub> pollution) as well as the associated O<sub>3</sub>-VOCs-NO<sub>x</sub> sensitivity. Therefore, one important concern for the policy formulation and implementation system is whether controlling VOCs and NO<sub>x</sub> individually or controlling both VOCs and NO<sub>x</sub> is more effective and appropriate for alleviating O<sub>3</sub> pollution. It is necessary to consider the reduction ratios of VOC/NO<sub>x</sub> when VOCs and NO<sub>x</sub> are simultaneously controlled. Finally, long-term monitoring studies are necessary to determine the cost-benefits and performance of each policy. To provide more accurate discussion on the controlling VOCs and NO<sub>x</sub> in a regional/local perspective, the following text has been added:

*“Last but not the least, though the present study suggested that reducing VOC emissions could be more effective in controlling O<sub>3</sub> pollution in the urban area of Nanjing where photochemical O<sub>3</sub> formation was VOC-limited, the results were based on local measurements, which likely presented a local perspective. However, O<sub>3</sub> pollution is a regional cross-boundary environmental issue rather than a local pollution problem. Apart from VOCs, NO<sub>x</sub> was another important precursor for O<sub>3</sub> formation with its dual roles in O<sub>3</sub> production (enhancing O<sub>3</sub> formation in non NO<sub>x</sub>-saturated environment and titrating O<sub>3</sub> in NO<sub>x</sub>-saturated environment). In other areas (i.e., the rural environment and/or the downwind areas of urban center in the same region) where the concentrations of NO<sub>x</sub> are low and/or there is a non NO<sub>x</sub>-saturated environment, the*

*situation may be different and controlling VOCs should be conducted cautiously (Ou, et al., 2016; Yuan et al., 2013; Zheng et al., 2010). Therefore, from a regional perspective, the benefits of VOCs control measures could be further evaluated with those of NO<sub>x</sub> (i.e., the appropriate ratios of VOC/NO<sub>x</sub> for the reduction of O<sub>3</sub> pollution) as well as the associated O<sub>3</sub>-VOCs-NO<sub>x</sub> sensitivity. Therefore, one important concern for the policy formulation and implementation system is whether controlling VOCs and NO<sub>x</sub> individually or controlling both VOCs and NO<sub>x</sub> is more effective and appropriate for alleviating O<sub>3</sub> pollution. It is necessary to consider the reduction ratios of VOC/NO<sub>x</sub> when VOCs and NO<sub>x</sub> are simultaneously controlled. Finally, long-term monitoring studies are necessary to determine the cost-benefits and performance of each policy.”*

For details, please refer to Lines 654-669, Page 23 in the revised manuscript.

#### Minor Comments

Line 19: It would be good to note that the measurements at JAES were conducted using GC.

Reply: Thanks for the reviewer’s suggestion. To highlight we use GC for the measurements, it has been revised as:

*“we conducted a one-year sampling exercise using a thermal desorption-GC (gas chromatography) system ….”*

For details, please refer to Lines 18-19, Page 1 in the revised manuscript.

Lines 23-24: Awkward phrasing, recommend saying "We identified VOC sources using positive matrix factorization and assessed their contributions to photochemical O<sub>3</sub> formation using an observation-based model employing the MCM".

Reply: Thanks for the comment. The sentence has been revised accordingly. For details, please refer to Lines 23-25, Page 1 in the revised manuscript.

Line 30: "control on" seems strong, given that other factors (e.g. meteorology) play a very important role. May suggest using "precursor to"

Reply: Thanks for the suggestion. We have revised it accordingly. For details, please

refer to Line 30, Page 1 in the revised manuscript.

Line 32-33: Do you mean that the contribution of biogenic emissions to O<sub>3</sub> was significantly lower than anthropogenic emissions? It would be useful to make this comparison.

Reply: Yes, by considering both the reactivity and abundance of VOC species, the contribution of biogenic emissions to O<sub>3</sub> pollution was significantly lower than anthropogenic emissions. The text has been revised as follows:

*“..... the contribution of biogenic emissions to O<sub>3</sub> pollution was significantly reduced and lower than vehicular and industrial emissions.”*

For details, please refer to Lines 33-34, Page 1 in the revised manuscript.

Lines 45-48: The word "associated" suggests that rapid economic growth occurred because of increases in pollution. Would recommend replacing associated with "Rapid economic growth has led to ..."

Reply: Thanks for the suggestion. The text has been revised accordingly. Please refer to Lines 46-47, Page 2 in the revised manuscript.

Line 56: "VOCs" should be singular, since it is used as an adjective here. Other instances of this are found sparsely throughout the text.

Reply: Thanks for pointing this out. It has been revised accordingly in the text. Furthermore, other instances have been double-checked and corrected.

Line 62: What do you mean by "industrial structure"? Does you mean that there is a high presence of industry in Ningbo?

Reply: Yes. Ningbo is a coastal city located on the southern wing of the Yangtze River Delta with a high presence of petrochemical industry. Since petrochemical industry is the leading industry in Ningbo, the results of source apportionment show that petrochemical industry is the main source of VOCs in Ningbo (Mo et al., 2015, 2016). The description for industries in Ningbo has been added as followed:

*“.....which is a coastal city located on the southern wing of the Yangtze River Delta with petrochemical industry as its lead industry (Mo et al., 2015, 2016).”*

For details, please refer to Lines 63-64, Page 2 in the revised manuscript.

Line 76: You could clarify here that you employ the entire MCM (v 3.2).

Reply: Thanks for pointing this out. It has been revised in the manuscript accordingly (Line 79, Page 3)

Line 78-79: Summarized, proposed, and assessed should be present tense here, since you are recommending these in the present manuscript.

Reply: Yes. It has been revised accordingly (Lines 81-82, Page 3).

Line 100: When you say "the sample was enriched after 600 mL of air sample" do you mean "600 mL of air was sampled"? If so, the latter phrasing may be more clear.

Reply: Thanks a lot for the comment. To clarify the sample collection, the text have been revised as follows:

*“The sampling flow was 15 mL/min. After 600 mL of air was sampled, the cold trap was heated to resolve the compounds adsorbed on to it.”*

For details, please refer to Lines 119-120, Page 4 in the revised manuscript.

Line 101: What is the “Dean’s Switch” technology?

Reply: Thanks for the comment. Dean’s Switch technology is the technology that transfers the effluent from one column to another column with a different stationary phase. By this technology, all co-eluting impurities in the target analyte and the transferred peak are completely eluted.

To introduce this technology, the following description was added:

*“.....By applying the Dean's Switch technology whereby the technology that transfers the effluent from one column to another column with a different stationary phase,.....”*

For details, please refer to Lines 120-121, Page 4 in revised manuscript.

Line 107: Was this a custom calibration standard, or a commercially available standard?



If commercially available, it would be good to quote the manufacturer. If prepared in-house, are there uncertainties in the VOC mixture?

Reply: Thanks for pointing this out. The VOC standard was purchased commercially.

The following description was added:

*“Seven analyses were performed repeatedly to test the precision of the 56 species. Calibrant concentrations in the gas standard mixture (56 C<sub>2</sub>-C<sub>12</sub> NMHCs, Linde Spectra Environment Gases, Inc, USA) ranged from 20 to 49 ppbC.”*

For details, please refer to Lines 128-129, Page 4 in the revised manuscript.

Line 245: “Identified” is a confusing word choice, since you identified the sources, not the model! I would recommend changing to “Five VOC sources were resolved by PMF”.

Reply: Thanks for the reviewer’s recommendation. It has been revised as suggested in Line 388, Page 13.

# Sources of volatile organic compounds and policy implications for regional ozone pollution control in an urban location of Nanjing, East China

Qiuyue Zhao<sup>1,2</sup>, Jun Bi<sup>1\*</sup>, Qian Liu<sup>2</sup>, Zhenghao Ling<sup>3\*</sup>, Guofeng Shen<sup>4</sup>, Feng Chen<sup>2</sup>, Yuezhen Qiao<sup>2</sup>, Chunyan Li<sup>2</sup>, Zongwei Ma<sup>1</sup>

<sup>1</sup>State Key Laboratory of Pollution Control and Resource Reuse, School of the Environment, Nanjing University, Nanjing 210023, China

<sup>2</sup>Jiangsu Key Laboratory of Environmental Engineering, Jiangsu Academy of Environmental Sciences, Nanjing 210036, China

<sup>3</sup>School of Atmospheric Sciences, Sun Yat-sen University, Guangzhou 510275, China

<sup>4</sup>College of Urban and Environmental Sciences, Peking University, Beijing 100871, China

Correspondence to: Jun Bi (jbi@nju.edu.cn) and Zhenhao Ling (lingzh3@mail.sysu.edu.cn)

**Abstract.** Understanding the composition, temporal variability, and source apportionment of volatile organic compounds (VOCs) is necessary for determining effective control measures to minimize VOCs and its related photochemical pollution. To provide a comprehensive analysis of VOC sources and their contributions to ozone (O<sub>3</sub>) formation in the Yangtze River Delta (YRD) - a region experiencing highest rates of industrial and economic development in China, we conducted a one-year sampling exercise using a thermal desorption-GC (gas chromatography) system for the first time at an urban site in Nanjing (JAES site). Alkanes were the dominant group at the JAES site, contributing ~53% to the observed total VOCs, followed by aromatics (~17%), acetylene (~17%), and alkenes (~13%). We identified seasonal variability in TVOCs with maximum and minimum concentrations in winter and summer, respectively. A morning and evening peak and a daytime trough were identified in the diurnal VOCs patterns. We identified VOC sources using positive matrix factorization and assessed their contributions to photochemical O<sub>3</sub> formation using an observation-based model employing the master chemical mechanism (MCM). The PMF model identified five dominant VOC sources, with highest contributions from diesel vehicular exhausts (34 ± 5%), followed by gasoline vehicular exhausts (27 ± 3%), industrial emissions (19 ± 2%), fuel evaporation (15 ± 2%) and biogenic emissions (4 ± 1%). The results from the OBM-MCM model simulation inferred photochemical O<sub>3</sub> formation to be VOC-limited at the JAES site when considering both the reactivity and abundance of the individual VOC species in each source category. Further, VOCs from vehicular and industrial emissions were found to be the dominant precursors to O<sub>3</sub> formation, particularly the VOC species *m,p*-xylene, toluene and propene, which top priorities should be given to the alleviation of photochemical smog. However, when considering the reactivity and abundance of VOC species in each source, the contribution of biogenic emissions to O<sub>3</sub> pollution was significantly reduced and lower than vehicular and industrial emissions. Our results therefore highlight the need to consider both the abundance and reactivity of individual VOC species in order to develop effective control strategies to minimize photochemical pollution in Nanjing.

## 37 **1. Introduction**

38 Volatile organic compounds (VOCs) are key precursors of O<sub>3</sub> and secondary organic aerosols (SOA) - a major  
39 component of fine particulate matter (PM<sub>2.5</sub>). VOCs significantly contribute to the formation of photochemical  
40 smog, atmospheric oxidative capacity, visibility degradation, and global climate (Jenkin and Clemitshaw, 2000;  
41 Seinfeld and Pandis, 2006), and some VOCs are also known to be toxic to human health. Therefore, in recent  
42 years, much research has focused on the impacts of VOCs due to their influence on atmospheric chemistry and  
43 impacts on human health (Shao et al., 2009 and references therein).

44  
45 The Yangtze River Delta (YRD) region (Shanghai-Jiangsu-Zhenjiang region) is one of the fastest growing  
46 regions in China, having recently undergone rapid urbanization and industrialization. [Rapid economic growth](#)  
47 has led to increased photochemical smog and elevated concentrations of ground-level O<sub>3</sub> and fine particulate  
48 matter (PM<sub>2.5</sub>). These conditions have been listed as the most important sources of pollution affecting the  
49 population in the YRD region, and are likely caused by increasing concentrations of VOCs. Therefore, it has  
50 been suggested that controlling VOC emissions is necessary for the effective alleviation of photochemical smog  
51 (Wang et al., 2009; Zhang et al., 2009; Cai et al., 2010; Kurokawa et al., 2013; Ding et al., 2016).

52  
53 To further understand VOC characteristics and to develop effective policies towards lowering VOC emissions,  
54 a number of sampling campaigns have been conducted to investigate the components, mixing ratios,  
55 photochemical reactivity and emissions of VOCs over the YRD region (Cai et al., 2010; An et al., 2014; Mo et  
56 al., 2015; Pan et al., 2015; Shao et al., 2016; Xu et al., 2017). For example, based on continuous observation data  
57 collected from March, 2011 to February, 2012, An et al. (2014) identified clear seasonal VOC variability in an  
58 industrial area of Nanjing, with maximum and minimum levels observed in summer and winter, respectively.  
59 VOC variability was also found to be strongly influenced by industrial emissions. In contrast, Mo et al. (2017)  
60 found no difference in VOC chemical compositions between residential, industrial and suburban areas of the  
61 coastal industrial city, Ningbo. By comparing the emission-based profiles and those extracted from the positive  
62 matrix factorization (PMF) model, the [petrochemical industry](#) was identified as the highest contributor of  
63 ambient VOCs due to the unique industrial structure of Ningbo, [which is a coastal city located on the southern](#)  
64 [wing of the Yangtze River Delta with petrochemical industry as its lead industry](#) (Mo et al., 2015, 2016). Pan et  
65 al. (2015) conducted emissions measurements of open biomass burning in the rural area of the YRD region and  
66 examined the major contributors to O<sub>3</sub> pollution using a box model together with the Regional Atmospheric  
67 Chemical Mechanism. Overall, these studies were conducted in industrialized and/or rural areas of the YRD  
68 region and demonstrate the contribution of industrial emissions and biomass burning towards ambient VOC  
69 levels and their contributions to O<sub>3</sub> formation. However, VOC studies in urban areas of the YRD region are  
70 limited and could help to improve our understanding of the spatial variability of VOCs and their environmental  
71 impact, particularly as stricter policies on VOCs and/or photochemical smog have been implemented since 2013

72 (Fu et al., 2016). Furthermore, the sampling resolution and sampling duration of these studies were relatively  
73 low as the samples were collected using canisters. High-resolution VOC datasets can provide more detailed  
74 information on the temporal and spatial variability, source apportionments, and impact factors of VOCs.

75

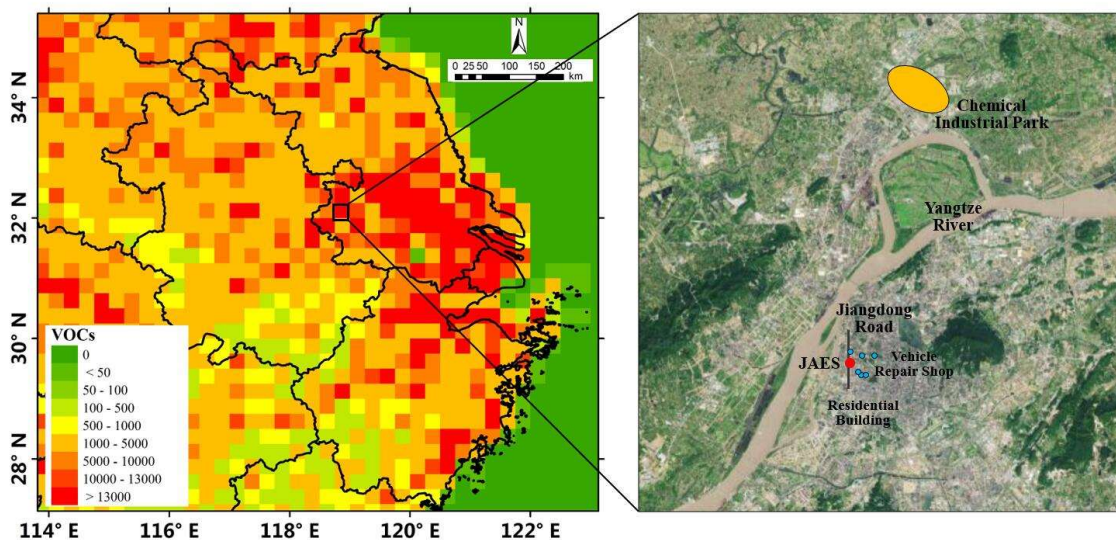
76 In this study, we collected continuous one-year observational VOC data at an urban site in Nanjing in the YRD  
77 region. The seasonal and diurnal characteristics of VOCs were investigated, and their sources were identified  
78 and quantified using the PMF model. Furthermore, we used a box model together with a Master Chemical  
79 Mechanism (MCM) (version 3.2) to identify the O<sub>3</sub>-precursor relationships and the contributions of VOC sources  
80 to photochemical O<sub>3</sub> formation. Our results were compared with VOCs data from other Chinese megacities.  
81 Based on these findings, we summarize and propose control strategies to minimize VOCs pollution and assess  
82 their implications for Nanjing and the wider YRD region. The results provide useful information towards  
83 lowering photochemical pollution in the YRD region as well as other regions in China.

## 84 2. Methodology

### 85 2.1. Sampling campaign

86 We continuously measured VOC concentrations from January to December, 2016, at an observation station on  
87 the rooftop of an office building (~80 m above the ground level) of the Jiangsu Academy of Environmental  
88 Science (JAES). There is a waterproof layer on the rooftop of the building but there was no guarantee that it was  
89 made of asphalt. Furthermore, despite this waterproof layer on the rooftop of the building, the interferences of  
90 emissions from this layer were believed to be insignificant because: 1) The waterproof layer was covered by the  
91 layer of concrete, which was further covered with a layer of ceramic tile; 2) The building had been built for three  
92 years before the sampling campaign was started; 3) It was documented that the VOC emitted from asphalt mainly  
93 included benzene, toluene, ethylbenzene and xylene (Gardiner and Lange, 2005). However, the levels of benzene,  
94 toluene, ethylbenzene, *m/p*-xylene and *o*-xylene were lower than those observed in other urban, industrial and  
95 rural environments in different regions (section 3.1, Zhang et al., 2012; An et al., 2014 and 2015; Mo et al., 2015,  
96 2017; He et al., 2019). 4) The sampling inlet was about 2-3 m above the rooftop of the building. It should be  
97 noted that there is a waterproof layer on the rooftop of the building. However, it is not sure that the waterproof  
98 layer was made of asphalt. Furthermore, though there is a waterproof layer on the rooftop of the building, the  
99 interferences of emissions from the layer were believed to be insignificant because: 1) The waterproof layer was  
100 covered by the layer of concrete, which was further covered with a layer of ceramic tile; 2) The building has  
101 been built for at least three years when the sampling campaign was started; 3) It was documented that the VOC  
102 emitted from asphalt mainly included benzene, toluene, ethylbenzene and xylene (Gardiner and Lange, 2005).  
103 However, the levels of benzene, toluene, ethylbenzene, *m/p*-xylene and *o*-xylene were lower than those observed  
104 in other urban and industrial and rural environments in different regions (Zhang et al., 2012; An et al., 2014 and  
105 2015; Mo et al., 2015, 2017; He et al., 2019) (details in section 3.1). 4) The sampling inlet were about 2-3 m

106 above the rooftop of the building. The station is located in an urban area of Nanjing, and is surrounded by heavy  
 107 road traffic, residential buildings, a plant and flower market, and several auto repair shops (Figure 1). Nanjing,  
 108 located in the western part of the YRD region, is one of the most urbanized and industrialized areas in the world  
 109 and consequently experiences severe air pollution. The site is located downwind of both Nanjing city center and  
 110 the wider YRD region (Zhao et al., 2017; Zhou et al., 2017), and is therefore ideally placed to determine the  
 111 combined impacts of VOCs from both local and regional atmospheric pollution.



112  
 113 **Figure 1. (a) Maps of the study location showing VOCs emission at a resolution of 0.25 degrees (MG/a) (The data were from**  
 114 **MEIC emission inventory (www.meicmodel.org, last access date: 15 September 2019). (b) The location of the JAES sampling**  
 115 **site is indicated by a red circle (The base map was from © Baidu Maps). The blue circles indicate vehicle repair shops, the**  
 116 **yellow circle indicates chemical industry park and the black solid line indicates a heavy traffic road**

117 Fifty-six VOC species including alkanes, alkenes, aromatics, and acetylene were measured at 1-h intervals using  
 118 a PerkinElmer Online Ozone Precursor Analyzer based on a thermal desorption-GC (gas chromatography)  
 119 system. First, the dried air samples were collected by a thermal desorption instrument and subsequently pre-  
 120 concentrated onto a cold trap. The sampling flow was 15 mL/min. After 600 mL of air was sampled, the cold  
 121 trap was heated to resolve the compounds adsorbed on to it. By applying the Dean's Switch technology whereby  
 122 the technology that transfers the effluent from one column to another column with a different stationary phase,  
 123 the low- and high-volatile components were injected into the Al<sub>2</sub>O<sub>3</sub>/Na<sub>2</sub>SO<sub>4</sub> PLOT column (50 m × 0.22 mm ×  
 124 1 μm) and the dimethyl siloxane column (50 m × 0.32 mm × 1 μm), respectively, and analyzed using a flame  
 125 ionization detector (FID). The temperature increased from 46 °C for 15 min to 170 °C at a rate of 5 °C/min, and  
 126 then to 200 °C at a rate of 15 °C/min. The samples were finally held at 200 °C for 6 min.

127  
 128 A calibration was performed daily for quality control. The calibration curves showed good linearity with a  
 129 correlation coefficient of 0.99. Seven analyses were performed repeatedly to test the precision of the 56 species.  
 130 Calibrant concentrations in the gas standard mixture (56 C<sub>2</sub>-C<sub>12</sub> NMHCs, Linde Spectra Environment Gases, Inc,  
 131 USA) ranged from 20 to 49 ppbC. The relative standard deviations of most of the 56 species were <5%,

132 representing an error of <0.5 ppb.

133 On the other hand, trace gases including CO, NO-NO<sub>2</sub>-NO<sub>x</sub>, SO<sub>2</sub>, and O<sub>3</sub> were measured at 1-min resolution  
134 using the commercial instruments of TEI 48i, 42i, 43i and 49i (Thermo Electron Corporation). All these  
135 instruments were zero checked daily, span calibrated weekly and multi-point calibrated monthly. Furthermore,  
136 meteorological conditions, including the temperature, relative humidity, pressure, wind speed and direction were  
137 monitored at 1-min resolution by a weather station (Vantage Pro TM & Vantage Pro 2 plus TM Weather Stations,  
138 Davis Instruments).

## 139 2.2. The PMF model for VOC source identification

140 In this study, the US EPA PMF (version 4.1) model, which has been widely used to conduct source apportionment  
141 of VOCs (Zhang et al., 2013; Mo et al., 2017; He et al., 2019 and references therein), was applied to the observed  
142 VOC data to identify potential VOC sources. A detailed description of the PMF model is provided by Yuan et al.  
143 (2009) and Ling et al. (2011). In brief, the PMF model is a receptor model, which can identify the sources and  
144 contributions of given species without prior input of their source profiles. In this study, a total of 25 species were  
145 selected as the input for the PMF model including species with high abundances as well as typical tracers of  
146 emission sources. Species with high percentages of missing values (> 25%) were excluded (i.e., 1,3-butadiene,  
147 cis/trans-2-pentene, dimethylpentane, and trimethylpentane). The total concentration of the 25 selected species  
148 accounted for ~92% of the total measured VOC composition. Furthermore, we calculated the total reactivity of  
149 the selected 25 species to be ~90% of the total measured VOCs through the analysis of maximum incremental  
150 reactivity (MIR) (Shao et al., 2009a). The high abundance and total reactivity contributions suggests that the  
151 selected 25 species were appropriate for the PMF model simulation.

152  
153 The PMF model was tested using a variety of factor numbers, and the optimum source profiles and contributions  
154 were determined based on the correlation between modelled and observed data, the comparison of modelled  
155 profiles with the results from emission-based measurements, and previous studies involving PMF/other receptor  
156 model simulations (i.e., HKEPD, 2015; Wang et al., 2014; An et al., 2014; Liu et al., 2008a). For example,  
157 different solution with different factor numbers was explored and the source apportionment results from a five-  
158 factor resolution that could sufficiently explain the observed levels of VOCs were selected (details in Section  
159 3.3). Compared with five-factor solution, the four-factor solution derived two profiles that attributable to gasoline  
160 and diesel vehicular exhaust, while most of the aromatic species in these sources and certain amounts of C<sub>3</sub>-C<sub>4</sub>  
161 species from fuel evaporation were categorized under industrial emission. On the other hand, the six-factor  
162 solution has split a factor with high presence of ethyne and certain amounts of ethane (30% in species total), C<sub>3</sub>  
163 species and benzene (~20% in species total), while some alkenes (18-80% in species total) were incorporated  
164 into fuel evaporation. Furthermore, the performance of the five-factor solution was evaluated using various  
165 checks and sensitivity tests. Suitable correlations between the observed concentrations and those of each species  
166 predicted by the model were observed, with the correlation coefficients (R<sup>2</sup>) ranging from 0.60 - 0.91, indicating

167 that the solution adequately reproduced the observed variations of each species. All the scale residuals were  
168 within  $\pm 3\sigma$  with normal distributions for all species (Baudic et al., 2016). Moreover, different numbers of start  
169 seeds were tested during the simulation and no-multiple solutions were found. The ratio of  $Q(\text{robust})/Q(\text{true})$   
170 obtained was  $\sim 0.93$ , close to 1 as suggested by previous studies and the user guide manual (Paatero, 2000; Lau  
171 et al., 2010; Ling et al., 2016). In addition, the results from bootstrapping analysis for the five-factor solution  
172 with bootstrap random seed found that all the factors were mapped to a basic factor in all the 20 bootstrap runs,  
173 while the uncertainties of each species from bootstrapping analysis were within the range of 1~20%. In this study,  
174 different  $F_{\text{peak}}$  values ranging from -5 to 5 was tested in the 5-factor solution for a more realistic profile (Lau et  
175 al., 2010; Baudic et al., 2016). The profiles with the nonzero  $F_{\text{peak}}$  values were consistent with those with zero  
176  $F_{\text{peak}}$  value, reflecting that there was little rotation for the selected solution, confirming that the profiles were  
177 reasonably explained by the five-factor solution (Baudic et al., 2016). The results of  $F_{\text{peak}}$  value = 0.5 (the base  
178 run) was selected for analysis in this study. Overall, the above features demonstrated that the five-factor solution  
179 from PMF could provide reasonable and stable apportionment results for the observed VOCs at the JAES site.

### 180 **2.3. VOC contributions on O<sub>3</sub> formation using the observation-based model**

181 In this study, we applied the observation-based model (OBM) coupled with the MCM (version 3.2)  
182 (<http://mcm.leeds.ac.uk/MCMv3.2/citation.htm>, Lyu et al., 2016; He et al., 2019), which consists of  $\sim 6000$   
183 reactions involving  $\sim 16,500$  species without considering vertical and horizontal transport, to quantify the  
184 contributions of VOC emission sources to photochemical O<sub>3</sub> formation. This model has been widely used to  
185 identify the photochemical reactivity and photochemical products in different environments (Volkamer et al.,  
186 2007; Xue et al., 2014a,b,c; Li et al., 2014; He et al., 2019). Detailed configurations of the model have been  
187 introduced in previous studies (Saunders et al., 2003; Lam et al., 2013). In this study, the hourly data of VOCs,  
188 trace gases (i.e., CO, NO<sub>x</sub>, SO<sub>2</sub>, and O<sub>3</sub>), and meteorological parameters (i.e., temperature, relative humidity,  
189 pressure and heights of boundary layer) on 88 O<sub>3</sub> episode days (identified as hourly maximum O<sub>3</sub> concentrations >  
190 80 ppbv per day) were used to constrain the model. In the model, the height of the boundary layer was configured  
191 to increase gradually from  $\sim 300$  m in the morning to  $\sim 1500$  m in the afternoon and then collapsed back to 300  
192 m at night based on the radiosonde and reanalysis data in China (Guo et al., 2016). On the other hand, as neither  
193 the photolysis of O<sub>3</sub> ( $J(\text{O}^1\text{D})$ ) nor that of NO<sub>2</sub> ( $J(\text{NO}_2)$ ) was measured in this study, the photolysis frequencies,  
194 including  $j(\text{O}^1\text{D})$ ,  $j(\text{NO}_2)$  and photolysis rates of other species were calculated using the photon flux determined  
195 from the Tropospheric Ultraviolet and Visible Radiation model (TUV, version 5.3,  
196 [http://cprm.acom.ucar.edu/Models/TUV/Interactive\\_TUV/](http://cprm.acom.ucar.edu/Models/TUV/Interactive_TUV/), access date: 03 Jan 2020) based on the actual  
197 conditions, such as solar radiation, location and time period of the field campaign in Nanjing. The  
198 parameterization for the scheme of the TUV (v5.3) module can be found in the code of MCM  
199 (<http://mcm.leeds.ac.uk/MCMv3.3.1/home.htm>, access date: 07 Jan 2010). Additional information on the model  
200 calculation and performance has been reported in the previous studies (Pinho et al., 2009; Lam et al., 2013; Shao  
201 et al., 2016; Wang et al., 2017). Figure S1 in the supplementary presented the mean diurnal pattern of  $J(\text{NO}_2)$

202 simulated by the OBM model using TUV scheme. A typical solar-driven diurnal cycle with the maximum value  
203 ( $\sim 11.1 \times 10^{-3} \text{ s}^{-1}$ ) at noon (1100-1200 LT) were observed in the photolysis of  $\text{J}(\text{NO}_2)$ , which was consistent with  
204 those observed and modelled in China (Li et al., 2011; Wang et al., 2019), suggesting that the simulated  
205 photolysis frequencies using the TUV scheme in the model was appropriate in the present study. To simulate  
206 each  $\text{O}_3$  episode day, we ran the model for two-days using the mean diurnal variability of the input species during  
207 the whole sampling period to achieve a steady state for the unmeasured mixing ratios of species with a short  
208 lifetime, i.e., OH and  $\text{HO}_2$  radicals (Wang et al., 2017; Sun et al., 2018).

209  
210 As the  $\text{O}_3$  simulated by the OBM was derived based on the observed mixing ratios of precursors and local  
211 meteorology, it is more appropriate to refer the simulation of  $\text{O}_3$  by the OBM as local produced  $\text{O}_3$ , though the  
212 observed mixing ratios of precursors could be both influenced by local emissions and those transported from  
213 upwind areas (Liu et al., 2019). Therefore, before using the isopleth calculation, it is necessary to investigate  
214 whether locally produced  $\text{O}_3$  from OBM could make a significant portion to the observed  $\text{O}_3$  at the JAES site.  
215 The investigation on the wind parameters found that the average wind speed was  $\sim 1.8$  m/s on  $\text{O}_3$  episode days,  
216 with about  $\sim 51\%$  of most wind speed data being  $\leq 2$  m/s (see Figure S2 in the supplementary), suggesting that  
217 regional transport may not have a significant influence on the levels of  $\text{O}_3$  and its precursors on episode days at  
218 the JAES site (Shao et al., 2016; Wang et al., 2017).

219  
220 Figure S3 in the supplementary showed the timeseries for the comparison between local produced  $\text{O}_3$  from OBM  
221 and the observed  $\text{O}_3$  mixing ratios, while Figure S4 in the supplementary presented the comparison between the  
222 mean diurnal variations of simulated and observed  $\text{O}_3$  mixing ratios for all the  $\text{O}_3$  episode days at the JAES site.  
223 It was found that the model underestimated or overestimated  $\text{O}_3$  on some episode days. The comparison between  
224 the mean diurnal variations of simulated and observed  $\text{O}_3$  suggested that the model captured the diurnal  
225 variations of  $\text{O}_3$ , and the predicted and observed maximum  $\text{O}_3$  values were comparable, though the predicted  
226 mixing ratios of  $\text{O}_3$  were lower than that observed in the early morning. The above discrepancy between observed  
227 and predicted  $\text{O}_3$  mixing ratios was mainly due to the failure to consider physical processes (i.e., horizontal and  
228 vertical transport) and/or the other  $\text{O}_3$  precursors (i.e., carbonyls and other oxygenated VOCs (OVOCs)) (Shao  
229 et al., 2009a; Cheng et al., 2010; Liu et al., 2019). However, the simulation indeed provided a reasonable  
230 description of the  $\text{O}_3$  variations using the observation data. To assess the local photochemically produced  $\text{O}_3$   
231 against the measured levels of  $\text{O}_3$  during the  $\text{O}_3$  episode days, the amount of the locally produced  $\text{O}_3$  formed by  
232 the photochemistry was compared with the observed  $\text{O}_3$  accumulations that were calculated as difference  
233 between the peak and early-morning concentrations of  $\text{O}_3$ . The amount of local photochemically produced  $\text{O}_3$   
234 was determined by the net  $\text{O}_3$  production rate, which was calculated by the difference between the gross  
235 production  $G(\text{O}_3)$  and destruction rates  $D(\text{O}_3)$  in the model (Equations 1-3).



$$P(O_3) = G(O_3) - D(O_3) \quad (1)$$

$$G(O_3) = k_{HO_2+NO}[HO_2][NO] + \sum k_{RO_2i+NO}[RO_{2i}][NO] \quad (2)$$

$$D(O_3) = k_{HO_2+O_3}[HO_2][O_3] + k_{OH+O_3}[OH][O_3] + k_{O(^1D)+H_2O}[O(^1D)][H_2O] \\ + k_{OH+NO_2}[OH][NO_2] + k_{alkenes+O_3}[alkenes][O_3] \quad (3)$$

237 Where the  $k$  constant values were the rate coefficients for the subscript reaction. The detailed description for the  
 238 above calculation was provided by Xue et al. (2013, 2014) and Wang et al. (2017). At JAES, the daytime (07:00–  
 239 19:00 LT) average net  $O_3$  production rate was estimated to be  $6.2 \text{ ppbv h}^{-1}$ , corresponding to  $\sim 74 \text{ ppbv } O_3$  formed  
 240 from local photochemistry during daytime hours. The amount was coincident with the average increment of  $O_3$   
 241 observed from early morning to late afternoon at JAES ( $\sim 81 \text{ ppbv}$ ), suggesting that local photochemically  
 242 produced  $O_3$  significantly contributed to the  $O_3$  increment at JAES. Indeed, the observed minimum  $O_3$  mixing  
 243 ratios before accumulation which were considered as the residual  $O_3$  levels (or background  $O_3$ , the mean value  
 244 was  $20 \text{ ppbv}$ ) at the sampling site as suggested by the previous studies (Xue et al., 2013, 2014a,b) only accounted  
 245 for  $\sim 20\%$  of the observed maximum  $O_3$  values (the mean value was  $102 \text{ ppbv}$ ) (data not shown). Furthermore,  
 246 the difference between observed and simulated minimum  $O_3$  mixing ratios which was considered as the fraction  
 247 of residual  $O_3$  that could not be explained by the OBM model only contributed  $\sim 17\%$  of the observed maximum  
 248  $O_3$  mixing ratio. The above analysis on the difference between observed and simulated  $O_3$  levels confirmed that  
 249 local photochemical produced  $O_3$  made a significant fraction to observed  $O_3$  levels at JAES. However, we  
 250 admitted that the OBM model could not accurately estimate the contributions of residual  $O_3$  to the increment of  
 251  $O_3$  values during daytime, which requires to be studied using a combination of different models and dataset (i.e.,  
 252 the regional air quality model, Lagrangian dispersion model and emission inventory) (Jiang et al., 2010; Ding et  
 253 al., 2013a, b; Wang et al., 2015).

254  
 255 To further evaluate the model performance, the index of agreement (IOA) that was developed to assess the  
 256 agreement between modelled and observed results was used in this study (Huang et al., 2005; Wang et al., 2013,  
 257 2015; Liu et al., 2019). The calculation of IOA was as follows:

$$IOA = 1 - \frac{\sum_{i=1}^n (O_i - S_i)^2}{\sum_{i=1}^n (|O_i - \bar{O}| + |S_i - \bar{O}|)^2} \quad (4)$$

259 Where  $S_i$  and  $O_i$  were the simulated and observed  $O_3$ , respectively, while  $\bar{O}$  was the mean of observed  $O_3$ , and  
 260  $n$  is the number of samples. The IOA values ranged between 0 and 1, and a relatively higher value of IOA  
 261 indicated relatively greater consistency between simulated results and observation data (Wang et al., 2013, 2015,  
 262 2017). In this study, the IOA of  $O_3$  was  $\sim 0.85$ , suggesting consistency of the abundance and variation of  $O_3$   
 263 between the observation and simulation, and demonstrating that locally produced  $O_3$  could be explained by the

264 measured precursors. Overall, the above analysis demonstrated that simulation of OBM could be used to conduct  
 265 O<sub>3</sub> isopleth calculation and investigate the O<sub>3</sub>-precursor relationship (Shao et al., 2016; Lyu et al., 2019; He et  
 266 al., 2019).

267  
 268 To investigate O<sub>3</sub>-precursor relationship, we used the model to calculate the relative incremental reactivity (RIR)  
 269 to assess the sensitivity of O<sub>3</sub> photochemical formation to changes in the concentrations of its precursors (Carter  
 270 and Atkinson, 1989; Cardelino and Chameides, 1995). The RIR is defined as the percent change in O<sub>3</sub> production  
 271 per percent change in precursors and is calculated as shown in Eq. (5), while the average RIR of precursor *X* is  
 272 calculated as shown in Eq. (6).

$$273 \quad RIR^S(X) = \frac{[P_{O_3-NO}^S(X) - P_{O_3-NO}^S(X-\Delta X)] / P_{O_3-NO}^S(X)}{\Delta S(X) / S(X)} \quad (5)$$

$$274 \quad \overline{RIR} = \frac{\sum_1^N [RIR^S(X) P_{O_3-NO}^S(X)]}{\sum_1^N P_{O_3-NO}^S(X)} \quad (6)$$

275 where the superscript *S* is the specific sample day; *S*(*X*) represents the measured concentration of precursor *X*,  
 276 including the amounts emitted at the site and those transported to the site; Δ*S*(*X*) is a hypothetical change in the  
 277 concentration of precursor *X* (10% *S*(*X*) in this study); and *N* is the number of evaluated days. *P*<sub>O<sub>3</sub>-NO</sub><sup>*S*</sup> is the O<sub>3</sub>  
 278 formation potential, which is the net O<sub>3</sub> production and NO consumed during the evaluation period.

279  
 280 Furthermore, to investigate the relative importance of the precursor species to photochemical O<sub>3</sub> formation, the  
 281 RIR-weighted values and the relative contributions of different precursors were calculated as shown in Eq. (7)  
 282 and Eq. (8), taking into consideration both the reactivity and abundance of VOC species (Ling et al., 2011; Ling  
 283 and Guo, 2014).

$$284 \quad RIR\text{-weighted}(X) = \overline{RIR}^X \times conc(X) \quad (7)$$

$$285 \quad Contribution(X) = \frac{\overline{RIR}^X \times conc(X)}{\sum [\overline{RIR}^X \times conc(X)]} \quad (8)$$

286 where *X* represents the specific precursor,  $\overline{RIR}^X$  is the average RIR value of precursor *X*, and *conc*(*X*) is the  
 287 concentration of precursor *X*.

## 288 3. Results and discussion

### 289 3.1 VOC observation statistics

290 Table 1 shows the average concentration and standard deviation of fifty-six VOC species concentrations  
 291 measured at the JAES site, while Figure S7 in the supplementary presented the time series of all pollution data  
 292 collected at the JAES site. The annual average total VOC (TVOC, sum of the measured VOCs) concentrations  
 293 in 2016 was 25.7 ± 19.1 ppbv, with highest contributions from alkanes (13.6 ± 10.5 ppbv, ~53%), followed by  
 294 aromatics (4.4 ± 4.0 ppbv, ~17%), acetylene (4.5 ± 5.5 ppbv, ~17%) and alkenes (3.2 ± 3.3 ppbv, ~13%).  
 295 Annually, the most abundant 10 species were acetylene, propane, ethane, ethylene, butane, toluene, *i*-pentane, *i*-

296 butane, propylene and benzene, with a combined contribution of ~77% of the TVOC. This observed VOC  
 297 composition suggests that VOCs at the JAES site are predominantly sourced from combustion emissions (i.e.,  
 298 vehicular emissions). Alkenes are mainly associated with vehicular emissions and are more photochemically  
 299 reactive relative to alkanes and aromatics. The alkenes were found to have higher mixing ratios [during weekdays](#)  
 300 [relative to the weekends](#) ( $3.5 \pm 0.2$  vs  $2.9 \pm 0.1$  ppbv for weekdays and weekend, respectively,  $p < 0.05$ ), further  
 301 confirming the dominant contribution of vehicular emissions to VOC levels at the JAES site.

302  
 303 **Table 1. The average mixing ratios and standard deviation of VOC species concentrations measured at the JAES site from**  
 304 **January to December 2016.**

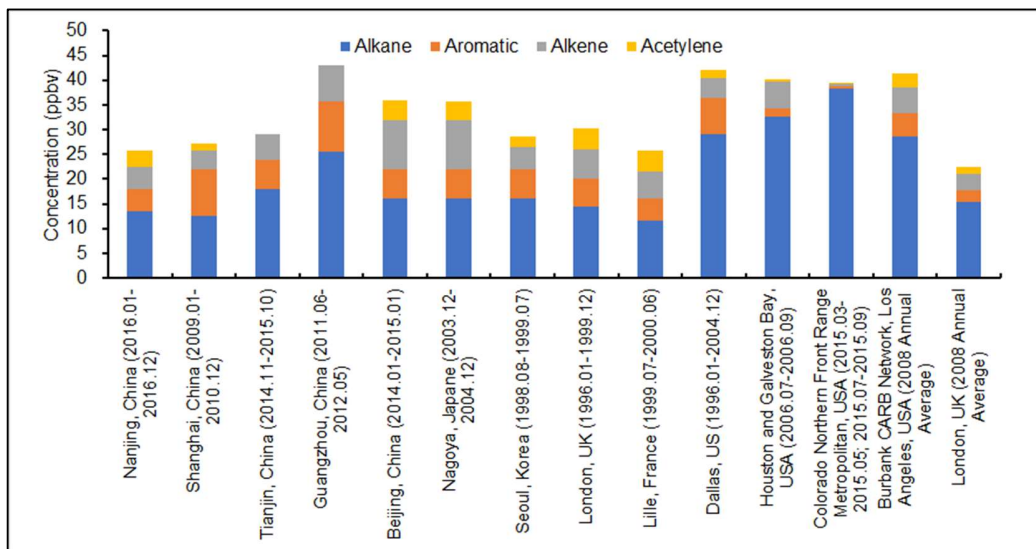
Species	Average $\pm$ Standard deviation (ppbv)	Species	Average $\pm$ Standard deviation (ppbv)
<b>Alkanes</b>	<b>13.64 <math>\pm</math> 10.53</b>	<b>Alkenes</b>	<b>3.24 <math>\pm</math> 3.28</b>
ethane	3.63 $\pm$ 2.68	ethene	1.72 $\pm$ 2.00
propane	3.70 $\pm$ 3.01	propylene	0.92 $\pm$ 1.16
<i>i</i> -butane	1.03 $\pm$ 0.87	1-butene	0.12 $\pm$ 0.16
<i>n</i> -butane	1.55 $\pm$ 1.26	<i>cis</i> -2-butene	0.06 $\pm$ 0.09
cyclopentane	0.08 $\pm$ 0.10	<i>trans</i> -2-butene	0.16 $\pm$ 0.11
<i>i</i> -pentane	1.15 $\pm$ 1.24	1-pentene	0.03 $\pm$ 0.03
<i>n</i> -pentane	0.61 $\pm$ 0.60	<i>cis</i> -1-pentene	0.02 $\pm$ 0.03
2,2-dimethylbutane	0.02 $\pm$ 0.02	<i>trans</i> -2-pentene	0.02 $\pm$ 0.03
2,3-dimethylbutane	0.05 $\pm$ 0.07	isoprene	0.14 $\pm$ 0.20
2-methylpentane	0.26 $\pm$ 0.29	<i>n</i> -hexene	0.05 $\pm$ 0.03
3-methylpentane	0.16 $\pm$ 0.21	<b>Aromatics</b>	<b>4.40 <math>\pm</math> 4.01</b>
<i>n</i> -hexane	0.40 $\pm$ 0.45	benzene	0.80 $\pm$ 0.70
methylcyclopentane	0.26 $\pm$ 0.27	toluene	1.40 $\pm$ 1.35
cyclohexane	0.10 $\pm$ 0.16	ethylbenzene	0.50 $\pm$ 0.62
2,4-dimethylpentane	0.03 $\pm$ 0.01	<i>m/p</i> -xylene	0.70 $\pm$ 0.71
2,3-dimethylpentane	0.03 $\pm$ 0.02	<i>o</i> -xylene	0.25 $\pm$ 0.24
2-methylhexane	0.06 $\pm$ 0.09	styrene	0.12 $\pm$ 0.17
3-methylhexane	0.07 $\pm$ 0.10	<i>n</i> -propylbenzene	0.03 $\pm$ 0.03
heptane	0.09 $\pm$ 0.11	<i>i</i> -propylbenzene	0.03 $\pm$ 0.04
methylcyclohexane	0.07 $\pm$ 0.09	<i>m</i> -ethyltoluene	0.11 $\pm$ 0.14
2,2,4-trimethylpentane	0.02 $\pm$ 0.03	<i>p</i> -ethyltoluene	0.05 $\pm$ 0.07
2,3,4-trimethylpentane	0.02 $\pm$ 0.01	<i>o</i> -ethyltoluene	0.04 $\pm$ 0.05
2-methylheptane	0.02 $\pm$ 0.02	1,3,5-trimethylbenzene	0.04 $\pm$ 0.06
3-methylheptane	0.02 $\pm$ 0.02	1,2,4-trimethylbenzene	0.15 $\pm$ 0.21
octane	0.04 $\pm$ 0.06	1,2,3-trimethylpentane	0.10 $\pm$ 0.14
nonane	0.02 $\pm$ 0.02	<i>m</i> -diethylbenzene	0.03 $\pm$ 0.06
decane	0.04 $\pm$ 0.04	<i>p</i> -diethylbenzene	0.04 $\pm$ 0.08
undecane	0.04 $\pm$ 0.07	<b>Acetylene</b>	<b>4.47 <math>\pm</math> 5.49</b>
dodecane	0.09 $\pm$ 0.20	--	--

305  
 306 The TVOC level in this study was lower than previous measurements from an industrial site in Nanjing, in which

307 43.5 ppbv TVOC was reported (An et al., 2014). However, the high TVOC levels are likely due to the proximity  
308 of the observation site (~3 km northeast) to the Nanjing chemical industry area, as well as several iron, steel, and  
309 cogeneration power plants (within 2 km) (An et al., 2014). The variability in land-use between these two studies  
310 have also resulted in distinct VOC component profiles. In the industrial area, the relative contributions of alkenes  
311 and aromatics were as high as 25% and 22%, while the contribution of alkynes was only 7% (An et al., 2014).  
312 The alkane, alkene, and aromatic concentrations from the industrial site were 1.4, 3.4, and 2.2 times higher than  
313 the concentrations of this study, respectively, while alkyne concentrations were ~30% lower. Given the large  
314 variability observed between the two sites, it is crucial to assess the spatial variability of ambient VOCs across  
315 the city through a collaboration of multiple research groups using available real-time and online VOC monitoring  
316 systems.

317  
318 Table S1 compares reported ambient VOCs from continuous measurements of  $\geq 1$  year in several megacities in  
319 a number of countries, including China. Continuous online measurements of ambient VOCs have only been  
320 available in China since 2010, unlike many developed countries [whereby online VOC measurements have been](#)  
321 [available for multiple decades](#). In China, such measurements are only concentrated in a few megacities, including  
322 Beijing, Guangzhou, and Shanghai. The TVOC level reported in Nanjing was close to levels measured in  
323 Shanghai (another megacity in the YRD, East China, 27.8 ppbv) (Wang et al., 2013), Tianjin (a megacity in  
324 North China, 28.7 ppbv) (Liu et al., 2016), and Wuhan (a megacity located in central China, 24.3 ppbv) (Lyu et  
325 al., 2016), but was considerably lower than Beijing (north China, 35.2 ppbv) (Zhang et al., 2017) and Guangzhou  
326 (south China, 42.7 ppbv) (Zou et al., 2015). Alkanes were the dominant hydrocarbon group in all the cities;  
327 however, some differences in relative contributions of the four classes were observed. The contribution from  
328 aromatics was highest in Shanghai (31%) relative to the other cities, which is likely explained by the large  
329 petrochemical and steel industry in Shanghai (Huang et al., 2011; Wang et al., 2013). In comparison, the  
330 contribution of aromatics in Guangzhou (Zou et al., 2015) and the industrial area in Nanjing (An et al., 2014)  
331 were 24% and 22%, respectively, while in other cities the contribution ranged between 17-19%. The current  
332 ambient VOC concentrations in Chinese megacities are generally comparable to the urban VOC levels in  
333 developed countries during the year 2000. [However, in developed countries, the mixing ratios of VOCs were](#)  
334 [observed to decrease in the recent decades following the implementation and formulation of VOC strategies](#)  
335 [\(Warneke et al., 2012\). For example, the mixing ratios of VOCs in Los Angeles have decreased significantly](#)  
336 [from 1960-2002 at an average annual rate of ~7.5%, while the mixing ratios of VOCs in London presented a](#)  
337 [higher and faster decreased since 1998 when there were higher VOC mixing ratios than those in Los Angeles,](#)  
338 [confirming that the earlier implementation of VOC reduction strategies in California had clearly led to the earlier](#)  
339 [improvement of air quality compared to London \(Warneke et al., 2012; von Schneidmesser et al., 2010\).](#)  
340 [Chinese megacities are therefore experiencing significantly higher ambient VOCs contamination, given the](#)  
341 [remarkable decrease in VOC emissions in developed countries over the last two decades \(Pan et al., 2015;](#)  
342 [European Environment Agency, 2016; U.S. EPA, 2017;\).](#) High VOC levels in Chinese megacities are known to

343 impact ambient ozone and secondary particle pollution, as well as cause adverse impacts on human health.  
 344 However, as China has a solid foundation for VOCs monitoring and control, numerous strict, appropriate and  
 345 targeted reduction strategies for VOCs have been/are being formulated and implemented in Chinese megacities  
 346 (Guo et al., 2017). It is expected these measures could help China to reduce VOC emissions/mixing ratios and  
 347 improve air quality in the future.



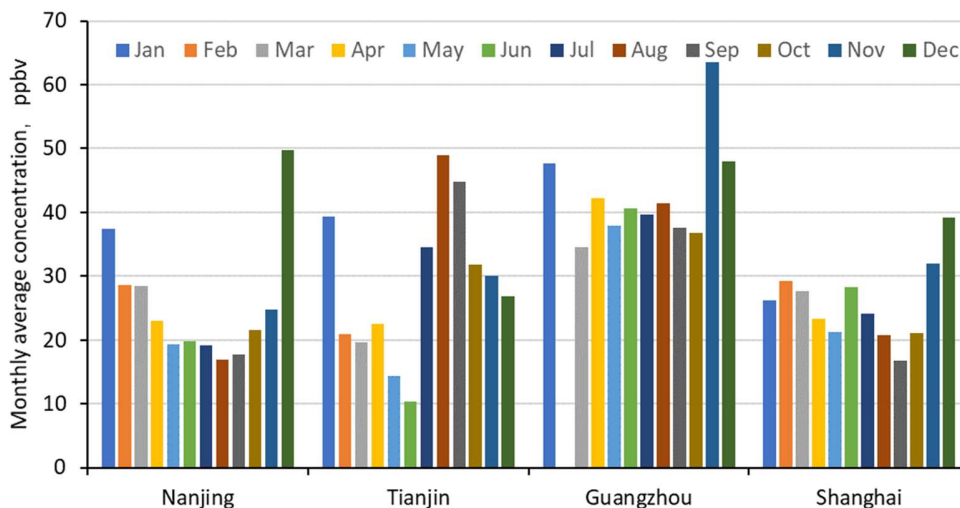
348  
 349 **Figure 2. Comparison of annual average concentrations of ambient VOC in different cities based on real-time online**  
 350 **continuous measurements of at least one year.**

351 **3.2 Temporal variability**

352 In this study, ambient VOCs showed significant seasonal variability, with relatively high monthly average  
 353 concentrations in winter ( $40.2 \pm 24.0$  ppbv) and spring ( $23.8 \pm 15.0$  ppbv), and low concentrations in summer  
 354 ( $18.5 \pm 14.6$  ppbv) and autumn ( $20.1 \pm 12.2$  ppbv). As shown in Figure S5, the highest monthly average  
 355 concentration was observed in December, followed by January. High pollution levels during the winter period  
 356 are usually expected and is explained by atmospheric temperature inversions caused by cooler weather, which  
 357 inhibits particle dispersion. Lower concentrations during the summer period are due to both favorable diffusion  
 358 conditions and photochemical degradation of VOCs.

359 High wintertime VOCs pollution were also reported in Shanghai (Wang et al., 2013), Guangzhou (Zou et al.,  
 360 2015), and Tianjin (Liu et al., 2016), though some differences in the monthly VOC variability were also observed.  
 361 Except for the winter months, similar (and relatively stable) ambient VOC levels in the remaining months were  
 362 observed for Guangdong (Figure 3). In Shanghai, relative high levels of VOCs were observed from October to  
 363 January of the following year and from June to July based on the two-year measurement conducted from 2009  
 364 to 2010 (Wang et al., 2013). The inversion layer, the effect of cold front or uniform pressure in winter resulted  
 365 in high levels of VOCs from October to January of the following year, while the frontal inverted trough or  
 366 frequently observed stagnant high pressure system with southwest flow that could lead to poor diffusion were  
 367

368 unfavorable meteorological conditions for high VOC levels from June to July. In addition, air masses transported  
 369 from upwind chemical and petrochemical industrial factories located in the southwest and south of the  
 370 monitoring site was another factor for the high VOC levels in summer (*i.e.*, June and July) and winter. VOCs  
 371 concentrations in Tianjin showed significant monthly variability. Highest concentrations were reported in  
 372 autumn and lowest concentrations were reported in summer. The observed monthly variability is affected by  
 373 several factors including the type and level of emissions and local meteorological conditions.



374  
 375 **Figure 3. Monthly variability of ambient VOCs at the JAES site and three other Chinese cities, Shanghai (Wang et al., 2013),**  
 376 **Guangzhou (Zou et al., 2015), and Tianjin (Liu et al., 2016).**

377 Figure S6 shows the diurnal trends in ambient VOCs for each month. The diurnal patterns were generally similar  
 378 for all the months. The observed peak at approximately 8-9 am (local time) corresponds with the city’s morning  
 379 traffic rush. The concentration begins to decrease after 9 am, with lowest concentrations observed at  
 380 approximately 3 pm. The observed decline was likely due to reduced vehicle emissions, growth of the inversion  
 381 top, and enhanced photochemical VOC degradation. After 3 pm, the concentrations begin to increase gradually  
 382 as a result of increased vehicle emissions during the evening rush hour, as well as a reduction in the atmospheric  
 383 mixing height under evening meteorological conditions. The second evening VOC peak was less prominent than  
 384 the morning peak. Evening concentrations were generally higher than the daytime concentrations, and the  
 385 amplitudes of diurnal variability were larger in autumn and summer compared to winter and spring.

386

### 387 3.3 Source apportionment of VOCs

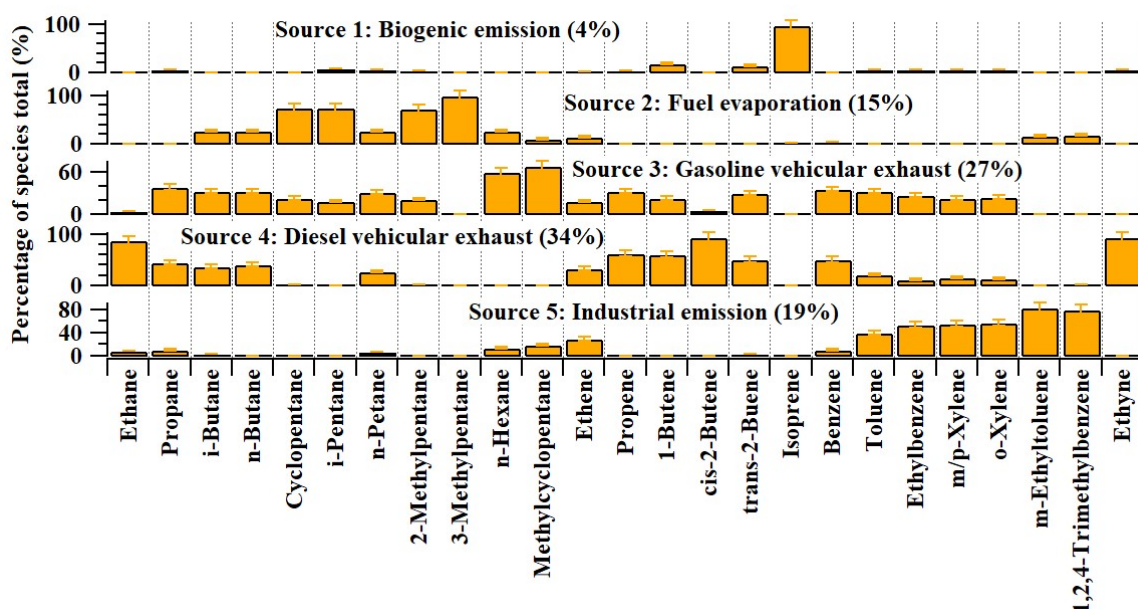
388 In this study, we applied the PMF model to apportion the sources of VOCs at the sampling site. Figure 4  
 389 illustrates the source profiles of the VOCs produced by the PMF model. Five VOC sources were resolved by  
 390 PMF, including biogenic emissions (Source 1), fuel evaporation (Source 2), gasoline vehicular exhausts (Source  
 391 3), diesel vehicular exhausts (Source 4), and industrial emissions (Source 5).

392

393 Source 1 was identified as biogenic emissions due to the high loading of isoprene – a typical tracer of biogenic  
394 emissions (Lau et al., 2010; Yuan et al., 2012). Source 2 was represented by high proportions of 2-methylpentane,  
395 3-methylpentane, *i*-pentane, and cyclopentane. Pentanes are mainly associated with profiles from gasoline-  
396 related emissions (Barletta et al., 2005; Tsai et al., 2006). However, the low contributions of incomplete  
397 combustion tracers in this profile suggested that the VOCs were sourced from fuel evaporation. The high  
398 presence of pentanes in this profile was consistent with the source profile of gasoline volatilization extracted  
399 from principal component analysis/absolute principal component scores (PCA/APCs) based on the observed  
400 VOC data collected in an industrial area of Nanjing (An et al., 2014), the source profile of gasoline evaporation  
401 from PMF at the suburban site and urban site in Beijing and Hong Kong (Yuan et al., 2009; Lau et al., 2010).  
402 Particularly, based on the emission-based measurement, Liu et al. (2008b) conducted source apportionments of  
403 VOCs in the Pearl River Delta region by the chemical mass balance (CMB) receptor model, which attributed the  
404 source with high loadings of *n/i*-pentanes, cyclopentane and 2/3-methylpentane as gasoline evaporation.  
405 Therefore, Source 2 here was identified as fuel evaporation.

406  
407 Source 3 and Source 4 were identified as vehicular exhausts due to their high loadings of incomplete combustion  
408 tracers, i.e., C<sub>2</sub>-C<sub>4</sub> alkanes and alkenes (Guo et al., 2011a, b; Zhang et al., 2018). Zhang et al. (2018) compared  
409 the VOC composition of vehicular emissions from Zhujiang Tunnel in 2014 and 2004 in the Pearl River Delta  
410 region with those from other tunnel measurements. C<sub>2</sub>-C<sub>4</sub> alkanes and alkenes were found to made the greatest  
411 contributions to the loading of VOCs emitted from vehicles in 2014. The higher proportions of *n/i*-pentane, *n*-  
412 hexane, and methylcyclopentane in Source 3 relative to Source 4 indicated VOCs sourced from gasoline  
413 vehicular exhausts (Liu et al., 2008b; Guo et al., 2011b; Zhang et al., 2018). Source 4 was identified as diesel  
414 vehicular exhausts due to the high percentages of ethyne, ethane, and propene, as well as C<sub>2</sub>-C<sub>4</sub> alkenes (Ho et  
415 al., 2009; Cai et al., 2010; Ou et al., 2015; Liu et al., 2008c). Source 5 was characterized by high concentrations  
416 of aromatics. In addition to gasoline vehicle emissions, industrial emission could be another important  
417 contributor to ambient aromatic hydrocarbons in the Yangtze River Delta, Pearl River Delta and North China  
418 Plain (Yuan et al., 2009; Zhang et al., 2013, 2014; An et al., 2014; Mo et al., 2015, 2017; He et al., 2019). The  
419 tunnel studies and emission-based measurement results found that aromatic hydrocarbons from gasoline vehicle  
420 exhaust were coherently emitted with pentanes, butenes, *n*-hexane, and cyclopentane, which were more  
421 consistent with the profile in source 3 mentioned above (Liu et al., 2008; Ho et al., 2009; Yuan et al., 2009;  
422 Zhang et al., 2018). Therefore, the absence of above species in source 5 indicated that this source could be related  
423 to industrial emission (Zhang et al., 2014). Particularly, the high presence of toluene, ethylbenzene, xylenes,  
424 ethyltoluene and trimethylbenzene was consistent with the emission-base measurement results conducted in  
425 paint and printing industries (Yuan et al., 2010) and manufacturing facilities (Zheng et al., 2013). On the other  
426 hand, the profile of high presence of aromatic hydrocarbons (C<sub>7</sub>-C<sub>9</sub> aromatics) and the certain amount of ethene,  
427 was also agree with the profiles measured in the areas dominated by industrial emissions in the Yangtze River  
428 Delta region (An et al., 2014; Shao et al., 2016; Mo et al., 2017). For example, An et al. (2014) reported that

429 toluene, ethylbenzene, xylenes, and trimethylbenzenes could be emitted from different industrial processes, and  
 430 identified that the factors with high loadings of these species as industrial production, solvent usage and  
 431 industrial production volatilization sources by PAC/APCS at the industrial area in Nanjing. On the other hand,  
 432 Mo et al. (2017) identified the factors with high concentrations of C<sub>7</sub>-C<sub>9</sub> aromatics and ethene as residential  
 433 solvent usage, chemical and paint industries and petrochemical industry with the PMF model applied to the data  
 434 collected in an industrialized coastal city of Yangtze River Delta region. To further identify source 3 and source  
 435 5, the ratio of toluene/benzene (T/B, ppbv/ppbv) in each profile was compared with those obtained from  
 436 emission-based measurements and tunnel study results (Zhang et al., 2018 and references therein). The ratios of  
 437 T/B were ~8.2 and ~1.2 for sources 5 and 3, respectively, and were consistent with those of “industrial processes  
 438 and solvent application”, and “roadside and tunnel study”, respectively (Zhang et al., 2018 and references  
 439 therein). This further confirmed that source 3 was related to gasoline vehicular exhaust, while source 5 was  
 440 associated with industrial emission.



441 Figure 4. Source profiles of VOCs identified using the PMF model and the relative contributions of the individual VOC  
 442 species.  
 443

444 Vehicular exhausts were found to be the most significant contributor to the TVOCs at the JAES site, with average  
 445 contributions of ~34% and ~27% for diesel and gasoline exhausts, respectively, followed by industrial emissions  
 446 (19%), fuel evaporation (~15%), and biogenic emissions (~4%). Our results are inconsistent with previous results  
 447 observed at industrial sites in Nanjing (An et al., 2014; Xia et al., 2014a). An et al. (2014) found that industrial  
 448 activities were the most significant source of VOCs, contributing 45%-63% (mainly aromatic VOCs), followed  
 449 by vehicle emission at 34%-50%. Similarly, Xia et al. (2014a) reported solvent usage and other industrial sources  
 450 to account for most (31%) of the VOCs in a suburban site in southwestern Nanjing, close in proximity to  
 451 Nanjing’s industrial zone. Fossil fuel/biomass/biofuel combustion were the second highest contributors at 28%,  
 452

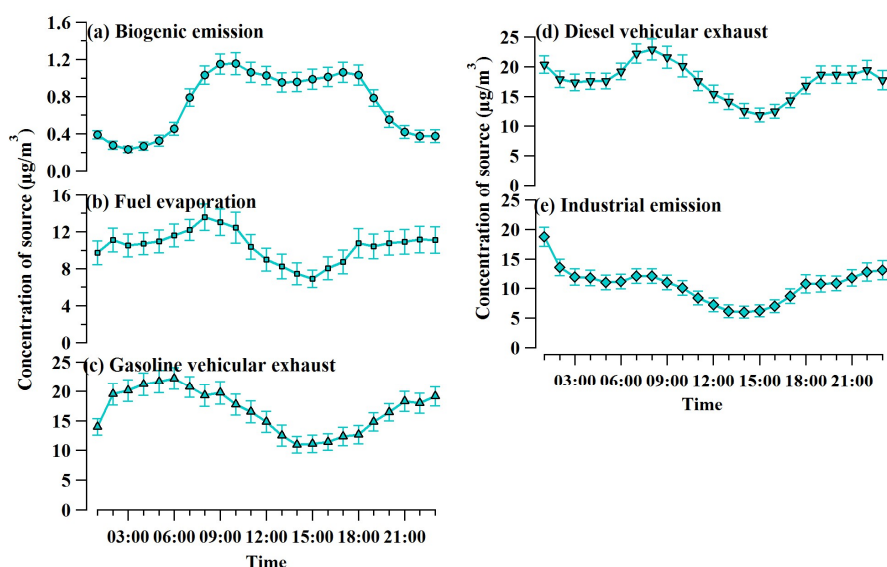


453 while the average contribution of vehicular emissions was 17%, mainly from the northern center of Nanjing (Xia  
454 et al., 2014a). Combined, these results infer vehicular emissions to be a major component of urban emissions in  
455 Nanjing. The observed spatial variability in the contributions of VOC sources infers the complex emissions  
456 characteristics of VOCs in Nanjing, likely due to the city's unique industrial structure. For example, the sampling  
457 site (i.e., the JAES site) was located at a more residential and urban area compared to other sites listed in An et  
458 al. (2014) and Xia et al. (2014). There are more than 0.22 million people living in the areas surrounding the  
459 sampled site (within 3 km of the observation site) which composed of residential communities, schools,  
460 government agencies, and business centers. These results also demonstrate that local emissions are dominant  
461 contributors to ambient VOCs levels in Nanjing.

462  
463 The dominant contribution of vehicular emissions to ambient VOCs in Nanjing is consistent with the  
464 urban/central areas of other large cities, including Hong Kong, Guangzhou, Shanghai, and Beijing, as identified  
465 and quantified by the PMF model (Yuan et al., 2009; Cai et al., 2010; Guo et al., 2011a; Zhang et al., 2013; Wang  
466 et al., 2015). In addition, our results are in agreement with the anthropogenic VOC source emission inventory of  
467 Jiangsu Province in 2010 (Xia et al., 2014b), indicating vehicular emissions and industrial emissions (i.e., solvent  
468 usage and industrial process source) to be the two dominant sources of VOCs in the region. However, the  
469 contributions of vehicle related emissions (i.e., ~25%) and industrial emissions were lower and higher than those  
470 quantified by the PMF model in this study, respectively. The observed discrepancy between the two studies may  
471 be due to differences in source categories, measured VOC species, and/or sampling locations and methods used  
472 in the different models. For example, the VOC sources in Jiangsu province were categorized into vehicular  
473 related emission (~26%), industrial solvent usage (~25%), fossil fuel combustion (~24%), industrial processes  
474 (~22%) and biomass burning (~3%). Further, vehicle related emissions only included emissions from motor  
475 vehicles and ships, and the volatilization of fuel, while solvent usage included organic solvents volatilized from  
476 a variety of industries (the industrial produce process of electronic equipment manufacturing, furniture  
477 manufacturing, printing, packaging, inks, adhesives, etc. and other dry cleaning, catering, and architectural  
478 decoration processes). Higher vehicular emission contribution in this study may also be due to the increasing  
479 number of vehicles from 2010-2014 as a result of increased urbanization and industrialization (Statistical  
480 yearbook of Nanjing, 2014).

481  
482 Figure 5 illustrates the mean diurnal variability of all identified source at the JAES site. These trends were  
483 influenced by the variability in emission strength, mixing height, and the concentrations and photochemical  
484 reactivity of individual species in each source profile. For example, we observed a typical diurnal pattern with a  
485 broad peak between 9 am-6 pm for biogenic emissions, as the emission rate of isoprene from vegetation is largely  
486 depended on ambient temperature and sunlight intensity. Higher levels of diesel and gasoline vehicular emissions  
487 were observed in the evening and early morning due to a reduced mixing height and increased emissions from  
488 the morning and evening rush hour. Lower concentrations observed during daytime hours were likely due to

489 decreased emissions, an increased mixing height and enhanced photochemical loss (Gillman et al., 2009; Yuan  
 490 et al., 2009; Wang et al., 2013). A diurnal pattern of fuel evaporation that was similar to that of vehicular  
 491 emissions. Though the evaporation of fuel is dependent on temperature, the average temperature in the morning  
 492 and evening (*i.e.*, 0800-1000 and 1700-1900 LT, respectively) when peaks of fuel evaporation were found was  
 493 only about  $\sim 1.2$  °C lower than that observed from noon to afternoon (1100-1600 LT), which may not result in  
 494 much higher fuel evaporation at noon (the difference between maximum and minimum values for fuel  
 495 evaporation was found to be  $\sim 6$   $\mu\text{g}/\text{m}^3$ ). On the other hand, in addition to evaporation from the gas station, fuel  
 496 could evaporate from hot engines, fuel tanks and the exhaust system when the car is running. Furthermore, the  
 497 engine remains hot for a period of time after the car is turned off, and gasoline evaporation continues when the  
 498 car is parked (Technology center, University of Illinois, <https://mste.illinois.edu/tcd/ecology/fuelevap.html>,  
 499 access date: 25 December 2019). The similarity of diurnal variations of fuel evaporation to vehicular emissions  
 500 suggested that the prominent peak in the morning and evening hours were related to the increased vehicles in  
 501 the traffic rush hour and emissions accumulated in the relatively low boundary layer. Moreover, we identified  
 502 higher concentrations of industrial emissions at night and in the early morning, with values remaining fairly  
 503 stable during daytime hours. This finding is consistent with other observations in urban and rural areas (Yuan et  
 504 al., 2009; Leuchner and Rappenglück, 2010).

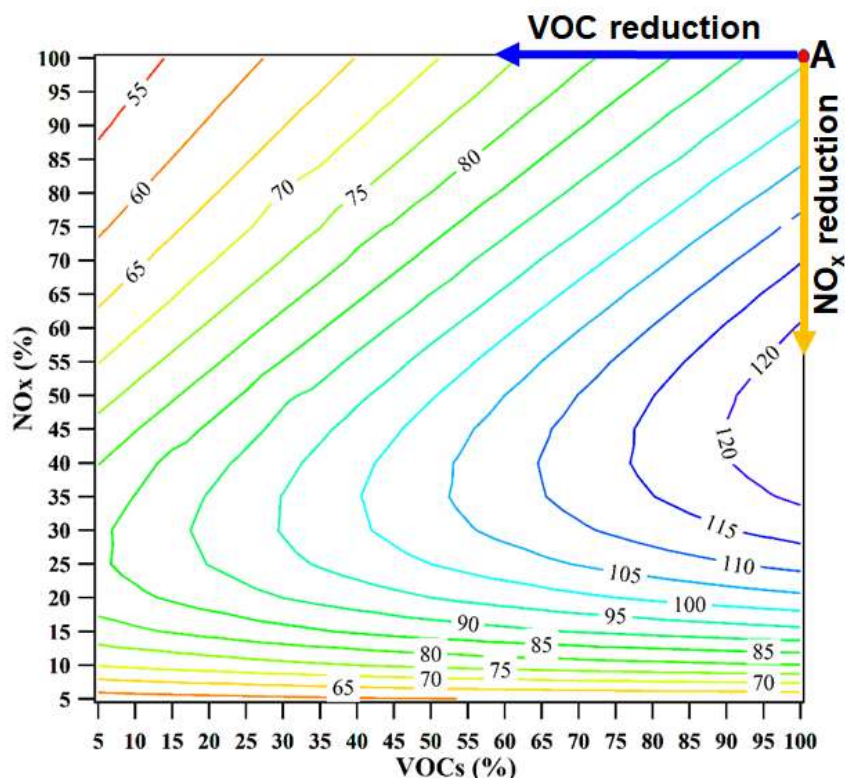


505  
 506 **Figure 5. Diurnal patterns in source concentrations of the five identified sources**

507 **3.4 Contributions of VOC sources to O<sub>3</sub> formation**

508 To highlight the relative contributions of the different emissions on VOC abundance during the 88 O<sub>3</sub> episode  
 509 days, we extracted and averaged the contributions of the different sources on these O<sub>3</sub> episode days from the  
 510 PMF model. It was found that the contributions of gasoline vehicular exhausts had significantly increased during  
 511 O<sub>3</sub> episode days, with a mean average percentage of  $41 \pm 5\%$ .

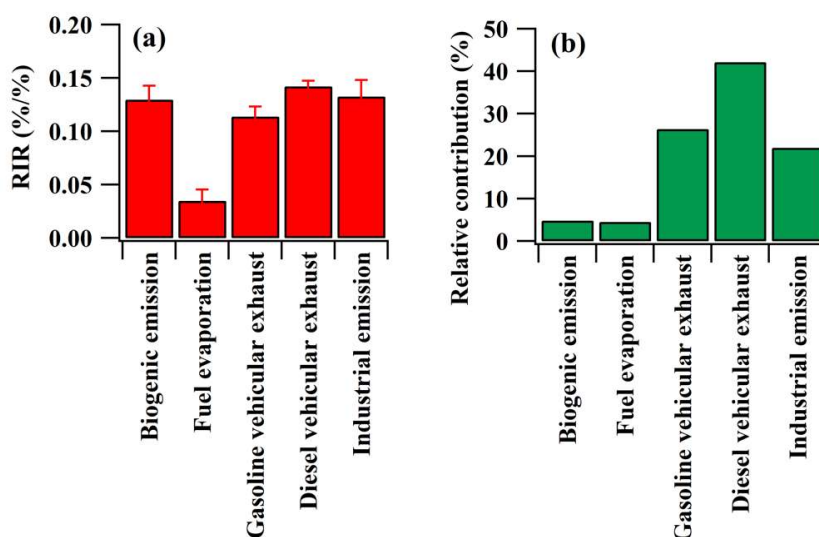
512 In the atmosphere, the sensitivity of photochemical O<sub>3</sub> formation was distributed into three regimes, including  
513 the VOC-limited regime, the NO<sub>x</sub>-limited regime and the transitional regime. In the VOCs-limited regime (the  
514 relative concentration [NO<sub>x</sub>]/[VOC] is high and/or NO<sub>x</sub> is saturated), photochemical O<sub>3</sub> formation decreases  
515 with the decrease in the concentration of VOCs (resulting from the control of VOC emissions), while in the NO<sub>x</sub>-  
516 limited regime (high [VOC]/[NO<sub>x</sub>] ratio and/or VOC is saturated), any reduction in the NO<sub>x</sub> concentration would  
517 shortens the O<sub>3</sub> formation chain length and reduces the photochemical O<sub>3</sub> formation (Jenkin and Clemitshaw,  
518 2000). The mean mixing ratios of NO<sub>x</sub> and TVOCs during daytime hours (0700-1800 LT, local time) on O<sub>3</sub>  
519 episode days were 19.2 ± 1.2 ppbv, respectively, with the mean ratio of VOCs/NO<sub>x</sub> as (ppbC/ppbv) ~3.4,  
520 suggested that the atmosphere in at the JAES site was NO<sub>x</sub> saturated and photochemical O<sub>3</sub> formation located in  
521 the VOC-regime (Jenkin and Clemitshaw, 2000). However, it should be noted that using the ratios of VOCs/NO<sub>x</sub>  
522 to determine the O<sub>3</sub> formation regime could be biased in different environments as different VOC species react  
523 at different rates and with different reaction mechanisms, thus inducing the nonlinear dependency of O<sub>3</sub>  
524 formation on NO<sub>x</sub> and VOCs. Figure 6 shows the O<sub>3</sub> isopleth plot illustrating the relationship between VOCs  
525 and NO<sub>x</sub> concentrations on the O<sub>3</sub> mixing ratio. The plot is the output from the OBM-MCM model, and is based  
526 on the mean diurnal variability of observed air pollutants on O<sub>3</sub> episode days. Based on the current scenario  
527 (with 100% of observed mixing ratios of VOCs and NO<sub>x</sub>, point A in Figure 6), the O<sub>3</sub> mixing ratio decreased  
528 with the reduction of VOCs and increased with the reduction of NO<sub>x</sub>, indicating that O<sub>3</sub> formation in this site is  
529 VOC-limited. Furthermore, to accurately evaluate the O<sub>3</sub>-precursor relationship, the RIR values from the OBM  
530 model, which were frequently used to evaluate the O<sub>3</sub> formation sensitivity based on observation data, were  
531 further explored. Positive RIR values were found for the VOCs (see Figure 7a), while negative values were  
532 found for NO<sub>x</sub> (i.e., -0.25 ± 0.02), further confirming that O<sub>3</sub> formation at the JAES site was VOC-limited (Zhang  
533 et al., 2008; Shao et al., 2009b; Cheng et al., 2010). In Figure 6, O<sub>3</sub> formation was found to be VOC-limited until  
534 NO<sub>x</sub> had decreased to a mixing ratio of 45%. Furthermore, O<sub>3</sub> formation becomes NO<sub>x</sub>-limited when the NO<sub>x</sub>  
535 mixing ratios are reduced by > 70%. Overall, the O<sub>3</sub> isopleth results suggest that minimizing VOC emissions  
536 would be effective at reducing O<sub>3</sub> formation at the JAES site.  
537



538  
539 **Figure 6.** The ozone isopleth in terms of the percentage change of VOCs and NO<sub>x</sub> (The horizontal and vertical axes  
540 correspond to the percentage of base-case VOCs and NO<sub>x</sub>, respectively). The ozone mixing ratios are in ppbv.

541 To further investigate the formulation and implementation of VOCs and their emissions, we simulated the RIR  
542 values of each source for all of the O<sub>3</sub> episode days using the OBM-MCM model (Figure 7). The RIR value  
543 represents the percentage change in O<sub>3</sub> production per percent change in the precursors. Positive RIR values  
544 indicate reduced O<sub>3</sub> formation with reduced source concentration, while negative values would indicate the  
545 opposite. A larger absolute RIR value indicates a stronger impact of a particular source on O<sub>3</sub> formation. Our  
546 results infer positive VOC RIR values and negative NO RIR values ( $-0.34 \pm 0.09$ ), indicating O<sub>3</sub> formation to  
547 be VOC-limited, which is consistent with the O<sub>3</sub> isopleth analysis. This observation is also consistent with  
548 previous results in industrial, traffic, residential and commercial areas of Nanjing (An et al., 2015; Zhang et al.,  
549 2018). However, the RIR values of each source were found to vary day-to-day due to the variability in the mixing  
550 ratios of VOCs and NO<sub>x</sub>, as well as changes in meteorological parameters. Figure 7a shows the mean RIR values  
551 of the different emission sources. Diesel vehicular exhausts were found to have the largest RIR value of  $0.14 \pm$   
552  $0.01$ , followed by industrial emissions ( $0.13 \pm 0.02$ ), biogenic emissions ( $0.12 \pm 0.01$ ), gasoline vehicle exhausts  
553 ( $0.11 \pm 0.01$ ), and fuel evaporation ( $0.03 \pm 0.01$ ). Therefore, VOC species in diesel vehicular exhausts and  
554 industrial emissions had the highest impact on O<sub>3</sub> photochemical formation at the JAES site. Furthermore, we  
555 calculated the relative contributions of the different sources based on the reactivity and abundance of individual  
556 VOC species. Our results showed that vehicle exhausts were the highest contributors to O<sub>3</sub> formation at ~68%,  
557 with diesel and gasoline vehicular exhausts contributing 42% and 26%, respectively. This was followed by

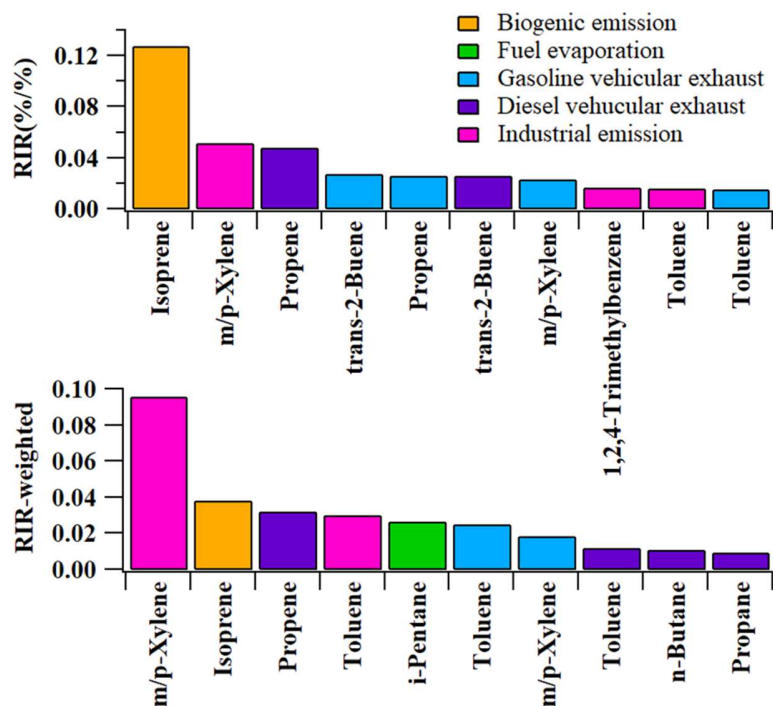
558 industrial emissions (22%), biogenic emissions (5%), and fuel evaporation (5%). Our results further demonstrate  
559 the need to minimize VOC emissions from vehicle exhausts in order to lower O<sub>3</sub> formation and photochemical  
560 pollution.



561  
562 **Figure 7a. The average RIR values of VOC sources, and (b) the relative contributions of different VOC sources to**  
563 **photochemical O<sub>3</sub> formation.**

564 To further investigate the relative importance of individual VOC species in each source, we calculated the RIR  
565 values and relative contributions of individual VOC species to photochemical O<sub>3</sub> formation. Figure 8 illustrates  
566 the 10 VOC species with highest RIR and RIR-weighted values at the JAES site. Based on the mass  
567 concentrations of individual species in each source, we found *m,p*-xylene and toluene in industrial emissions and  
568 gasoline vehicular emissions, propene and toluene in diesel vehicular emissions, and *i*-pentane in fuel  
569 evaporation to be the dominant species contributing to photochemical formation in each VOC source. Thus, only  
570 a small number of VOC species can be monitored for effective control of local O<sub>3</sub> formation. Though the  
571 photochemical reactivity of *i*-pentane, propane and *n*-butane were lower than alkenes and aromatics, their high  
572 RIR-weighted values indicate that high concentrations of VOCs with low photochemical reactivity can still  
573 significantly contribute to O<sub>3</sub> formation. This finding further confirms that both VOC reactivity and abundance  
574 should be considered for effective control of O<sub>3</sub> formation. Isoprene in biogenic emissions also shows high RIR-  
575 weighted values when considering both its reactivity and abundance. Currently, the majority of the VOC control  
576 measures are focused on anthropogenic emissions, yet the contributions of biogenic emissions on O<sub>3</sub> formation  
577 are also significant (section 3.5). This feature highlights the need to minimize VOCs from biogenic emissions  
578 for effective control of O<sub>3</sub> formation.

579



580 Figure 8. The average RIR values and RIR-weighted values of the top 10 VOC species in the different source categories.  
 581

### 582 3.5 Policy summary and implications

583 To effectively control photochemical pollution, the Prevention and Control of Atmospheric Pollution Act was  
 584 passed in 1987 and amended in 2015. As a result, a series of measures to prevent and control VOCs levels have  
 585 been and are being implemented by central and local governments, including the implementation of new laws  
 586 and regulations, and the advancement of technology. The results of this study suggest that photochemical O<sub>3</sub>  
 587 formation within the urban areas of Nanjing city are VOC-limited, which is consistent with observations in the  
 588 urban locations of other regions, including the North China Plain, the Yangtze River Delta and the Pearl River  
 589 Delta. Minimizing VOC emissions and their concentrations should therefore be prioritized in order to alleviate  
 590 O<sub>3</sub> pollution in urban environments. The prevention and control of VOC pollution has been listed as one of the  
 591 key tasks of “the Blue Sky” Project initiated in 2012 by the Department of Environmental Protection of Jiangsu  
 592 Province. Furthermore, the administrative measures on the Prevention and Control of Volatile Organic  
 593 Compounds Pollution in Jiangsu (Order No. 119 of the Provincial Government) was enacted on March 6, 2018  
 594 and implemented on May 1, 2018, with the aim of controlling VOC emissions in Jiangsu Province.

595 In order to achieve these goals, various measures have been implemented (Table S2), including: 1) investigating  
 596 the current pollution status and identifying the progress of VOC prevention and control in Jiangsu Province  
 597 (Provincial Office of the Joint Conference on the prevention and control of air pollution [2012] No. 2); 2)  
 598 conducting a strict industry access system, under the Advice on Promoting Air Pollution Joint Prevention and  
 599

600 Control Work to Improve Regional Air Quality (Office of the State Council [2010] No. 33); 3) strengthening the  
601 remediation on existing sources of VOCs and reducing VOC emissions from these sources, under the Guidelines  
602 for the Implementation of Leak Detection and Repair (LDAR) in Jiangsu Province (Trial) (Provincial Office of  
603 Environmental Protection [2013] No. 318); 4) strengthening the VOC monitoring capacity, under the Guidelines  
604 for Control of Volatile Organic Compounds Pollution in Key Industries in Jiangsu Province (Provincial Office  
605 of Environmental Protection [2013] No. 128); 5) improving standards regarding VOC emissions for key  
606 industries, including standards for surface coating of the automobile manufacturing industry (DB32/2862-2016),  
607 the chemical industry (DB32/3151-2016), and furniture manufacturing operations (DB32/3152-2016), which are  
608 still effective since their enforcement; 6) implementing the Pilot Measures for Volatile Organic Compounds  
609 Discharge Charges (Ministry of Finance [2015] No. 71) on October 1, 2015 to raise awareness pertaining to  
610 emissions reduction in factories and to control VOC emissions from industrial sources; 7) encouraging the public  
611 to live a low-carbon life and supervise and offer recommendations in accordance with the laws, under the  
612 Measures for Public Participation in Environmental Protection in Jiangsu Province (Trial) (Provincial Regulation  
613 of Environmental Protection Office [2016] No. 1).

614  
615 Based on the VOC source apportionment results in this study, we identified vehicular emissions and industrial  
616 emissions as the two major VOC sources contributing to photochemical O<sub>3</sub> formation. Other measures and/or  
617 regulations have been conducted in the Jiangsu Province to effectively control VOC emissions from vehicles  
618 and industry. For vehicular emissions, the Regulations on Prevention and Control of Vehicle Exhaust Pollution  
619 in Nanjing was amended in July 2017, and subsequently in March, 2018  
620 (<http://hbt.jiangsu.gov.cn/col/col11590/index.html>). The new regulation not only focusses on vehicle emissions,  
621 but also incorporates a number of additional topics, including optimizing the function and distribution of urban  
622 areas, limiting the number of vehicles in the region, promoting new green energy vehicles, and improving the  
623 quality of fuel. The promotion of intelligent traffic management, implementation of a priority strategy for public  
624 transportation, and construction of more efficient traffic systems to promote pedestrian and bicycle use is  
625 recommended. Further studies should be conducted to estimate and manage the increasing quantity of vehicles  
626 on the road. As of January 1, 2017, regulation stipulate that all new and used vehicles should meet the fifth phase  
627 of vehicle emission standards, including vehicle manufacture, sales, registration and importation. For vehicles  
628 already in use, an environmental protection examination should be conducted annually, based on the standards  
629 of GB 14622-2016, GB 18176-2016, GB 19755-2016, and HJ 689-2014. Penalties are issued if qualified  
630 vehicles excessively emit pollutants due to poor maintenance.

631  
632 For industrial emissions, various policies have been implemented to reduce VOC emissions, particularly in  
633 chemical industries: including, 1) investigations on the VOC emissions of the chemical industry and the  
634 establishment of an archive system for VOC pollution control, particularly the inspection of industry information,  
635 products and materials, unorganized emission of storage and exhaust gas treatment facilities, under the Plan for

636 Investigation of Volatile Organic Pollutant Emissions in Jiangsu Province, mentioned in the Provincial Office of  
637 Environmental Protection [2012] No. 183; 2) exhaust gas remediation in the chemical industry park, under the  
638 Technical Specifications for Prevention and Control of Air Pollution in Chemical Industries in Jiangsu Province  
639 (Provincial Office of Environmental Protection [2014] No. 3), which requires the establishment of the long-term  
640 supervision of exhaust gas remediation in the chemical industry park of Jiangsu Province; 3) a pilot project on  
641 the leak detection and repair (LDAR) technology in the chemical industry park, under the notification on carrying  
642 out the technical demonstration and pilot work of leak detection and repair (LDAR) in petrochemical and  
643 chemical industries (Provincial Office of Environmental Protection [2015] No. 157). The TVOC removal  
644 efficiency of organic exhaust vents should be >95%, and higher for areas of excessive environmental pollution  
645 at >97% (GB 31571-2015).

646  
647 Furthermore, though measures have been adopted to improve standards and control vehicle VOC emissions,  
648 most of these policies only focus on total VOC emissions (or the mass of total emissions) and do not consider  
649 the impacts of individual VOC species. To accelerate the implementation of existing policies and to strengthen  
650 collaborative regional prevention and control, priority should be placed on specific high-impact VOC species  
651 (i.e., *m,p*-xylene and toluene in the industrial emission and gasoline vehicular emission) by considering both  
652 their reactivity and abundance.

653  
654 Last but not the least, though the present study suggested that reducing VOC emissions could be more effective  
655 in controlling O<sub>3</sub> pollution in the urban area of Nanjing where photochemical O<sub>3</sub> formation was VOC-limited,  
656 the results were based on local measurements, which likely presented a local perspective. However, O<sub>3</sub> pollution  
657 is a regional cross-boundary environmental issue rather than a local pollution problem. Apart from VOCs, NO<sub>x</sub>  
658 was another important precursor for O<sub>3</sub> formation with its dual roles in O<sub>3</sub> production (enhancing O<sub>3</sub> formation  
659 in non NO<sub>x</sub>-saturated environment and titrating O<sub>3</sub> in NO<sub>x</sub>-saturated environment). In other areas (i.e., the rural  
660 environment and/or the downwind areas of urban center in the same region) where the concentrations of NO<sub>x</sub>  
661 are low and/or there is a non NO<sub>x</sub>-saturated environment, the situation may be different and controlling VOCs  
662 should be conducted cautiously (Zheng et al., 2010; Yuan et al., 2013; Ou, et al., 2016). Therefore, from a  
663 regional perspective, the benefits of VOCs control measures could be further evaluated with those of NO<sub>x</sub> (i.e.,  
664 the appropriate ratios of VOC/NO<sub>x</sub> for the reduction of O<sub>3</sub> pollution) as well as the associated O<sub>3</sub>-VOCs-NO<sub>x</sub>  
665 sensitivity. Therefore, one important concern for the policy formulation and implementation system is whether  
666 controlling VOCs and NO<sub>x</sub> individually or controlling both VOCs and NO<sub>x</sub> is more effective and appropriate for  
667 alleviating O<sub>3</sub> pollution. It is necessary to consider the reduction ratios of VOC/NO<sub>x</sub> when VOCs and NO<sub>x</sub> are  
668 simultaneously controlled. Finally, long-term monitoring studies are necessary to determine the cost-benefits  
669 and performance of each policy.



#### 670 4. Conclusion

671 In this study, a one-year field sampling campaign was conducted to investigate the VOC characteristics at an  
672 urban site in Nanjing (the JAES site), Jiangsu province. In total, 56 VOCs including 29 alkanes, 10 alkenes, 16  
673 aromatics and acetylene were identified and quantified. The composition analysis found that alkanes were the  
674 dominant group of VOCs observed at the JAES site (~53%), followed by aromatics, acetylene, and alkenes. This  
675 finding is consistent with the VOC measurements in studies conducted in the North China Plain, Pearl River  
676 Delta, and Yangtze River Delta. We observed distinct seasonal patterns of TVOCs, with maximum values in  
677 winter and minimum values in summer. Similarly, prominent morning and evening peaks were observed in the  
678 diurnal variability of TVOCs, influenced by local emissions and meteorology.

679  
680 Based on the observed VOC data, we identified five dominant VOC sources at the JAES site using a PMF model.  
681 By considering both the abundance and reactivity of individual VOC species in each source, the OBM-MCM  
682 model identified vehicular and industrial emissions, particularly *m,p*-xylene, toluene and propene, as the main  
683 contributors of O<sub>3</sub> pollution. Our results demonstrate that O<sub>3</sub> formation at the JAES site is VOC-limited and is  
684 predominantly controlled by a small number of VOC species. Local governments have strengthened several  
685 measures to minimize VOC pollution from vehicle and industrial emissions in the Jiangsu province in recent  
686 years, though most of these policies focus particularly on lowering the total emissions of VOCs. However, our  
687 results highlight the need to consider both the abundance and reactivity of individual VOC species in order to  
688 formulate effective control strategies to minimize pollution. Furthermore, from a regional perspective, it is  
689 suggested that appropriate ratios of VOC/NO<sub>x</sub>, their associated sensitivity to O<sub>3</sub> formation and relative  
690 benefits/disbenefits of reducing VOCs/NO<sub>x</sub> should be investigated and evaluated when control measures of  
691 VOCs and NO<sub>x</sub> were both conducted.

692

693 **Author Contributions.** Jun Bi, Zhenhao Ling, and Qiuyue Zhao designed the research and carried them out.  
694 Zhenhao Ling performed the data simulation. Qiuyue Zhao and Guofeng Shen performed the observation data  
695 analysis. Qiuyue Zhao prepared the manuscript with contributions from all co-authors.

696 **Competing Interests.** The authors declare that they have no conflict of interest.

697 **Acknowledgements.** This work was supported by National Key R&D Program of China (No.2016YFC0207607,  
698 2017YFC0210106), National Science Foundation of Jiangsu Province of China (General Program, No.  
699 BK20161601), Open Research Fund of Jiangsu Province Key Laboratory of Environmental Engineering  
700 (No.ZX2016002) and National Natural Science Foundation of China (No. 41775114). This work was also partly  
701 supported by the Pearl River Science and Technology Nova Program of Guangzhou (grant no. 201806010146).  
702 We thank Prof. Hai Guo of Hong Kong Polytechnic University for providing the MCM scheme to evaluate the  
703 relationship of O<sub>3</sub> and its precursors.

#### 704 Reference

- 705 An, J., Zhu, B., Wang, H., Li, Y., Lin, X., and Yang, H.: Characteristics and source apportionment of VOCs  
706 measured in an industrial area of Nanjing, Yangtze River Delta, China, *Atmospheric Environment*, 97, 206-  
707 214, 2014
- 708 An, J., Zou, J., Wang, J., Lin, X., and Zhu, B.: Differences in ozone photochemical characteristics between the  
709 megacity Nanjing and its suburban surroundings, Yangtze River Delta, China, *Environmental Science and*  
710 *Pollution Research International*, 22(24), 19607, 2015.
- 711 Barletta, B., Meinardi, S., Rowland, F.S., Chan, C.Y., Wang, X.M., Zou, S.C., Chan, L.Y. and Blake, D.R.:  
712 Volatile organic compounds in 43 Chinese cities, *Atmos. Environ.*, 39 (32), 5979-5990, 2005.
- 713 Baudic, A., Gros, V., Sauvage, S., Locoge, N., Olivier, S., Sarda-Estève, R., Kalogridis, C., Petit, J.-E., Bonnaire,  
714 N., Baisnee, D., Favez, O., Albinet, A., Sciare, J. and Bonsang, B.: Seasonal variability and source  
715 apportionment of volatile organic compounds (VOCs) in the Paris megacity (France), *Atmospheric*  
716 *Chemistry and Physics*, 16, 11961-11989, 2016.
- 717 Cai, C. J., Geng, F. H., Tie, X.X., and An, J. L.: Characteristic and source apportionment of VOCs measured in  
718 Shanghai, China, *Atmospheric Environment*, 44, 5005-5014, 2010.
- 719 Cardelino, C. A., and Chameides W. L.: An observation-based model for analyzing ozone precursor relationships  
720 in the urban atmosphere, *Air and Waste Management Association*, 45, 161–180, 1995.
- 721 Carter, W.L., and Atkinson, R.: Computer modeling study of incremental hydrocarbon reactivity, *Environmental*  
722 *Science and Technology* 23, 864-880, 1989.
- 723 Cheng, H.R., Guo, H., Wang, X.M., Saunders, S.M., Lam, S.H.M., Jiang, F., Wang, T., Ding, A., Lee, S. and Ho,  
724 K.F.: On the relationship between ozone and its precursors in the Pearl River Delta: application of an  
725 observation-based model (OBM), *Environmental Science and Pollution Research*, 17, 547-560, 2010.
- 726 Ding, A.J., Fu, C.B., Yang, X.Q., Sun, J.N., Zheng, L.F., Xie, Y.N., Herrmann, E., Nie, W., Petäjä, T., Kerminen,  
727 V.-M. and Kulmala, M.: Ozone and fine particle in the western Yangtze River Delta, an overview of 1 yr  
728 data at the SORPES station, *Atmospheric Chemistry and Physics*, 13, 5813-5830, 2013a.
- 729 Ding, A.J., Nie, W., Huang, X., Chi, X.G., Xu, Z., et al.: Ozone in the western Yangtze River Delta of China: a  
730 synthesis study based on ground, aircraft and sounding measurement 2011-2015, The 6th PEEEX meeting,  
731 May 2016, 2016
- 732 Ding, A.J., Wang, T. and Fu, C.B.: Transport characteristics and origins of carbon monoxide and ozone in Hong  
733 Kong, South China, *Journal of Geophysical Research*, 118, doi: 10.1002/jgrd.50714, 2013b.
- 734 Fu, L., Wan, W., Zhang, W., and Cheng, H.: Air pollution prevention and control progress in Chinese cities,  
735 *Clean Air Asia, China*, available at: [http://cleanairasia.org/wp-content/uploads/2016/08/China-Air-2016-](http://cleanairasia.org/wp-content/uploads/2016/08/China-Air-2016-Report-Full.pdf)  
736 [Report-Full.pdf](http://cleanairasia.org/wp-content/uploads/2016/08/China-Air-2016-Report-Full.pdf), 2016, last access: 16 May 2018.

737 Gardiner, M.S. and Lange, C.R.: Comparison of laboratory generated and field-obtained HMA VOCs with odour  
738 potential, *The International Journal of Pavement Engineering*, 6, 257-263, 2005.

739 Gilman, J.B., Kuster, W.C., Goldan, P.D., Herndon, S.C., Zahniser, M.S., Tucker, S.C., Brewer, W.A., Lerner,  
740 B.M., Williams, E.J., Harley, R.A., Fehsenfeld, F.C., Warneke, C. and de Gouw, J.A.: Measurements of  
741 volatile organic compounds during the 2006 TexAQSGoMACCS campaign: industrial influences, regional  
742 characteristics, and diurnal dependencies of the OH reactivity, *Journal of Geophysical Research*, 114,  
743 D7, doi: 10.1029/2008JD011525, 2009.

744 Guo, H., Cheng, H. R., Ling, Z. H., Louie, P. K. K., and Ayoko, G. A.: Which emission sources are responsible  
745 for the volatile organic compounds in the atmosphere of Pearl River Delta?, *Journal of Hazardous Materials*,  
746 188, 116-124, 2011a.

747 Guo, H., Zheng J. Y., Characterisation of VOC sources and integrated photochemical ozone analysis in Hong  
748 Kong and the Pearl River Delta region. Report to the Environmental Protection Department of Hong Kong  
749 (Tender Reference AS12-02909), Department of Civil and Environmental Engineering, The Hong Kong  
750 Polytechnic University, 2016.

751 Guo, H., Zou, S. C., Tsai, W. Y., Chan, L. Y., and Blake, D. R.: Emission characteristics of non-methane  
752 hydrocarbons from private cars and taxis at different driving speeds in Hong Kong, *Atmos. Environ.*, 45,  
753 2711–2721, 2011b.

754 Guo, J.P., Miao, Y.C., Zhang, Y., Liu, H., Li, Z.Q., Zhang, W.C., He, J., Lou, M.Y., Yan, Y., Bian, L.G. and Zhai,  
755 P.M.: The climatology of planetary boundary layer height in China derived from radiosonde and reanalysis  
756 data, *Atmospheric Chemistry and Physics*, 16, 13309-13319, 2016.

757 He, Z., Wang, X., Ling, Z., Zhao, J., Guo, H., Shao, M., and Wang, Z.: Contributions of different anthropogenic  
758 volatile organic compound sources to ozone formation at a receptor site in the Pearl River Delta region and  
759 its policy implications, *Atmos. Chem. Phys.*, 19, 8801-8816, 2019.

760 HKEPD (Hong Kong Environmental Protection Department): Characterisation of VOC sources and integrated  
761 photochemical ozone analysis in Hong Kong and the Pearl River Delta region. Final report, , Hong Kong,  
762 2015.

763 Ho, K.F., Lee, S.C., Ho, W.K., Blake, D.R., Cheng, Y., Li, Y.S., Ho, S.S.H., Fung, K., Louie, P.K.K. and Park,  
764 D.: Vehicular emission of volatile organic compounds (VOCs) from a tunnel study in Hong Kong,  
765 *Atmospheric Chemistry and Physics*, 9, 7491-7504, 2009.

766 Huang, C., Chen, C. H., Li, L., Cheng, Z., Wang, H. L., Huang, H. Y., Streets, D. G., Wang, Y. J., Zhang, G. F.,  
767 and Chen, Y.R.: Emission inventory of anthropogenic air pollutants and VOC species in the Yangtze River  
768 Delta region, China. *Atmos. Chem. Phys.*, 11, 4105-4120, 2011a

769 Huang, J.P., Fung, J.C.H., Lau, A.K.H. and Qin, Y.: Numerical simulation and process analysis of typhoon-related  
770 ozone episodes in Hong Kong, *Journal of Geophysical Research*, 110, D05301, doi:10.1029/2004JD004914,  
771 2005.

772 Jenkin, M. E. and Clemitshaw, K. C.: Ozone and other secondary photochemical pollutants: chemical processes  
773 governing their formation in the planetary boundary layer, *Atmospheric Environment*, 34, 2499-2527, 2000.

774 Jiang, F., Guo, H., Wang, T.J., Cheng, H.R., Wang, X.M., Simpson, I.J., Ding, A.J., Saunders, S.M., Lam, S.H.M.  
775 and Blake, D.R.: An ozone episode in the Pearl River Delta: field observation and model simulation, *Journal*  
776 *of Geophysical Research*, 115, D22, doi: 10.1029/2009JD013593, 2010.

777 Kurokawa, J., Ohara, T., Morikawa, T., Hanayama, S., Janssens-Maenhout, G., Fukui, T., Kawashima, K., and  
778 Akimoto, H.: Emissions of air pollutants and greenhouse gases over Asia regions during 2000-2008:  
779 Regional Emission inventory in Asia (REAS) version 2, *Atmos. Chem. Phys.*, 13, 11019-11058, 2013.

780 Lam, S. H. M., Saunders, S. M., Guo, H., Ling, Z. H., Jiang, F., Wang, X. M., and Wang, T. J.: Modelling VOC  
781 source impacts on high ozone episode days observed at a mountain summit in Hong Kong under the  
782 influence of mountain-valley breezes. *Atmos. Environ.*, 81, 166–176, 2013

783 Lau, A. K. H., Yuan, Z., Yu, J. Z., and Louie, P. K.: Source apportionment of ambient volatile organic compounds  
784 in Hong Kong, *Science of the Total Environment*, 408, 4138–4149, 2010.

785 Leuchner, M. and Rappenglück, B.: VOC source-receptor relationships in Houston during TexAQSGoMACCS-II,  
786 *Atmospheric Environment*, 44, 4056-4067, 2010.

787 Li, J., Wang, Z.F., Wang, X., Yamaji, K., Takigawa, M., Kanaya, Y., Pochanart, P., Liu, Y., Irie, H., Hu, B.,  
788 Tanimoto, H. and Akimoto, H.: Impacts of aerosols on summertime tropospheric photolysis frequencies  
789 and photochemistry over Central Eastern China, *Atmospheric Environment* 45, 1817-1829, 2011.

790 Li, X., Rohrer, F., Brauers, T., Hofzumahaus, A., and Wahner, A.: Modeling of HCHO and CHOCHO at a semi-  
791 rural site in southern China during the PRIDE-PRD 2006 campaign, *Atmos. Chem. Phys.*, 14, 33013-33054,  
792 2014.

793 Ling, Z. H., and Guo, H.: Contribution of VOC sources to photochemical ozone formation and its control policy  
794 implication in Hong Kong, *Environmental Science and Policy*, 38(3), 180-191, 2014.

795 Ling, Z. H., Guo, H., Cheng, H. R., and Yu, Y. F.: Sources of ambient volatile organic compounds and their  
796 contributions to photochemical ozone formation at a site in the Pearl River Delta, southern China,  
797 *Environmental Pollution*, 159, 2310-2319, 2011.

798 Liu, B., Liang, D., Yang, J., Dai, Q., Bi, X., and Feng, Y., Yuan, J., Xiao, Z.M., Zhang, Y.F., Xu, H.:  
799 Characterization and source apportionment of volatile organic compounds based on 1-year of observational  
800 data in Tianjin, China. *Environmental Pollution*, 218, 757-769 2015.

801 Liu, X., Lyu, X., Wang, Y., Jiang, F. and Guo, H.: Intercomparison of O<sub>3</sub> formation and radical chemistry in the  
802 past decade at a suburban site in Hong Kong, *Atmospheric Chemistry and Physics* 19, 5127-5145, 2019.

803 Liu, Y., Shao, M., Fu, L. L., Lu, S. H., Zeng, L. M., and Tang, D. G.: Source profiles of volatile organic  
804 compounds (VOCs) measured in China: Part I, *Atmospheric Environment* 42, 6247-6260, 2008a.

805 Liu, Y., Shao, M., Lu, S., Chang, C. C., Wang, J. L. and Fu, L.: Source apportionment of ambient volatile organic  
806 compounds in the Pearl River delta, China: part II, *Atmospheric Environment*, 42(25), 6261-6274, 2008b.

807 Liu, Y., Shao, M., Lu, S., Chang, C., Wang, J. L., and Chen, G.: Volatile organic compound (VOC) measurements  
808 in the Pearl River delta (PRD) region, China, *Atmos. Chem. Phys.*, 7(5), 1531-1545, 2008c.

809 Lyu, X., Chen, N., Guo, H., Zhang, W., Wang, N., Wang, Y., and Liu, M.: Ambient volatile organic compounds  
810 and their effect on ozone production in Wuhan, central China, *Science of the Total Environment*, 548-  
811 549(60), 483-483, 2016.

812 Lyu, X.P., Wang, N., Guo, H., Xue, L.K., Jiang, F., Zeren, Y.Z., Cheng, H.R., Cai, Z., Han, L.H. and Zhou, Y.:  
813 Causes of a continuous summertime O<sub>3</sub> pollution event in Jinan, a central city in the North China Plain,  
814 *Atmospheric Chemistry and Physics* 19, 3025-3042, 2019.

815 Mo, Z., Shao, M., and Lu, S.: Compilation of a source profile database for hydrocarbon and OVOC emissions  
816 in China, *Atmospheric Environment*, 143, 209-217, 2016.

817 Mo, Z., Shao, M., Lu, S. H., Niu, H., Zhou, M. Y., Sun, J.: Characterization of non-methane hydrocarbons and  
818 their sources in an industrialized coastal city, Yangtze River Delta, China, *Science of the Total Environment*,  
819 593-594, 641-653, 2017.

820 Mo, Z., Shao, M., Lu, S., Qu, H., Zhou, M., and Gou, B.: Process-specific emission characteristics of volatile  
821 organic compounds (VOCs) from petrochemical facilities in the Yangtze River Delta, China, *Science of the*  
822 *Total Environment*, 533, 422-431, 2015.

823 Ou, J., Guo, H., Zheng, J., Cheung, K., Louie, P. K. K., Ling, Z., and Wang D. W.: Concentrations and sources  
824 of non-methane hydrocarbons (NMHCs) from 2005 to 2013 in Hong Kong: a multi-year real-time data  
825 analysis, *Atmospheric Environment*, 103(103), 196-206, 2015.

826 Ou, J.M., Yuan, Z.B., Zheng, J.Y., Huang, Z.J., Shao, M., Li, Z.K., Huang, X.B., Guo, H. and Louie, P.K.K.:  
827 Ambient ozone control in a photochemically active region: short-term despiking or long-term attainment?  
828 *Environmental Science and Technology*, 50, 5720-5728, 2016.

829 Pan, X., Kanaya, Y., Tanimoto, H., Inomata, S., Wang, Z., Kudo, S., and Uno, I.: Examining the major  
830 contributors of ozone pollution in a rural area of the Yangtze River Delta region during harvest season,  
831 *Atmos. Chem. Phys.*, 15, 6101-6111, 2015

832 Pinho, P.G., Lemos, L.T., Pio, C.A., Evtuygina, M.G., Nunes, T.V. and Jenkin, M.E.: Detailed chemical analysis  
833 of region-scale air pollution in western Portugal using an adapted version of MCM v3.1, *Science of the*  
834 *Total Environment*, 407, 2024-2038, 2009.

835 Saunders, S. M., Jenkin, M. E., Derwent, R. G., and Pilling, M. J.: Protocol for the development of the Master  
836 Chemical Mechanism, MCM v3 (Part A): tropospheric degradation of nonaromatic volatile organic  
837 compounds, *Atmos. Chem. Phys.*, 3, 161-180, 2003.

838 Seinfeld, J. H. and Pandis, S. N.: *Atmospheric Chemistry and Physics: from air pollution to climate change*, 2nd  
839 edition. Wiley Publisher, New Jersey, USA, 2006.

840 Shao, M., Lu, S., Liu, Y., Xie, X., Chang, C., Huang, S., and Chen, Z.: Volatile organic compounds measured in  
841 summer in Beijing and their role in ground-level ozone formation, *Journal of Geophysical Research*, 114,  
842 D00G06, doi: 10.1029/2008JD010863, 2009a.

843 Shao, M., Zhang, Y.H., Zeng, L.M., Tang, X.Y., Zhang, J., Zhong, L.J. and Wang, B.G.: Ground-level ozone in  
844 the Pearl River Delta and the roles of VOC and NO<sub>x</sub> in its production, *Journal of Environmental*  
845 *Management*, 90, 512-518, 2009b.

846 Shao, P., An, J.L., Xin, J.Y., Wu, F.K., Wang, J.X., Ji, D.S. and Wang, Y.S.: Source apportionment of VOCs and  
847 the contribution to photochemical ozone formation during summer in the typical industrial area in the  
848 Yangtze River Delta, China, *Atmospheric Research*, 176-177, 64-74, 2016.

849 Song, Y., Dai, W., Shao, M., Liu, Y., Lu, S. H., Kuster, W., and Goldan, P.: Comparison of receptor models for  
850 source apportionment of volatile organic compounds in Beijing, China, *Environmental Pollution*, 156, 174-  
851 183, 2008.

852 Statistical yearbook of Nanjing, Nanjing Statistic Bureau:  
853 <http://221.226.86.104/file/nj2004/2014/jiaotongyunshu/index.htm>, last access: 17 May 2018, 2014

854 Sun, J.J., Li, Z.Y., Xue, L.K., Wang, T., Wang, X.F., Gao, J., Nie, W., Simpson, I.J., Gao, R., Blake, D. R., Chai,  
855 F. H., and Wang, W.X.: Summertime C1-C5 alkyl nitrates over Beijing, northern China: spatial distribution,  
856 regional transport, and formation mechanisms, *Atmospheric Research*, 204, 102-109. 2018.

857 Tasi, W.Y., Chan, L.Y., Blake, D.R. and Chu, K.W.: Vehicular fuel composition and atmospheric emissions in  
858 South China: Hong Kong, Macau, Guangzhou, and Zhuhai, *Atmospheric Chemistry and Physics*, 6, 3281-  
859 3288, 2006.

860 Volkamer, R., San Martini, F., Molina, L. T., Salcedo, D., Jimenez, J. L., and Molina, M. J.: A missing sink for  
861 gas-phase glyoxal in Mexico City: Formation of secondary organic aerosol, *Geophysical Research Letters*,  
862 34, 255-268, 2007.

863 von Schneidmesser, E., Monks, P.S. and Plass-Duelmer, C.: Global comparison of VOC and CO observations  
864 in urban areas, *Atmospheric Environment*, 44, 5053-5064, 2010.

865 Wang, H. L., Lou, S. R., Huang, C., Qiao, L. P., Tang, X. B., Chen, C. H., Zeng, L. M., Wang, Q., Zhou, M., Lu,  
866 S. H., and Yu, X.N.: Source profiles of volatile organic compounds from biomass burning in Yangtze River  
867 Delta, China, *Aerosol and Air Quality Research*, 14, 818-828, 2014

868 Wang, H., Chen, C., Wang, Q., Huang, C., Su, L., Huang, H., Lou, S., Zhou, M., Li, L., Qiao, L., and Wang, Y.:  
869 Chemical loss of volatile organic compounds and its impact on the source analysis through a two-year  
870 continuous measurement, *Atmospheric Environment*, 80, 488-498, 2013.

871 Wang, M., Shao, M., Chen, W., Lu, S., Liu, Y., Yuan, B., and Li, Y.: Trends of non-methane hydrocarbons  
872 (NMHCs) emissions in Beijing during 2002-2013, *Atmos. Chem. Phys.*, 15, 1489-1502, 2015.

873 Wang, N., Guo, H., Jiang, F., Ling, Z.H. and Wang, T.: Simulation of ozone formation at different elevations in  
874 mountainous area of Hong Kong using WRF-CMAQ model, *Science of the Total Environment*, 505, 939-  
875 951, 2015.

876 Wang, T., Wei, X. L., Ding, A. J., Poon, C. N., Lam, K. S., Li, Y. S., Chan, L. Y., and Anson, M.: Increasing  
877 surface ozone concentrations in the background atmosphere of Southern China, 1994–2007, *Atmos. Chem.*  
878 *Phys.*, 9, 6217-6227, 2009.

879 Wang, W.J., Li, X., Shao, M., Hu, M., Zeng, L.M., Wu, Y.S. and Tan, T.Y.: The impact of aerosols on photolysis  
880 frequencies and ozone production in Beijing during the 4-year period 2012-2015, *Atmospheric Chemistry*  
881 *and Physics*, 19, 9413-9429, 2019.

882 Wang, X.M., Liu, H., Pang, J.M., Carmichael, G., He, K.B., Fan, Q., Zhong, L.J., Wu, Z.Y. and Zhang, J.P.:  
883 Reductions in sulfur pollution in the Pearl River Delta region, China: assessing the effectiveness of emission  
884 controls, *Atmospheric Environment*, 76, 113-124, 2013.

885 Wang, Y., Wang, H., Guo, H., Lyu, X., Cheng, H., Ling, Z., Louie P., Simpson, I., Meinardi, S., Blake, D., : Long-  
886 term O<sub>3</sub>-precursor relationships in Hong Kong: field observation and model simulation, *Atmos. Chem.*  
887 *Physics.*, 17(18), 10919-10935, 2017.

888 Warneke, C., de Gouw, J.A., Holloway, J.S., Peischl, J., Ryerson, T.B., Atlas, E., Blake, D., Trainer, M. and  
889 Parrish, D.D.: Multiyear trends in volatile organic compounds in Los Angeles, California: Five decades of  
890 decreasing emissions, *Journal of Geophysical Research*, 117, D00V17, doi: 10.1029/2012JD017899, 2012.

891 Xia, L., Cai, C., Zhu, B., An, J., Li, Y., and Li, Y.: Source apportionment of VOCs in a suburb of Nanjing, China,  
892 in autumn and winter, *Journal of Atmospheric Chemistry*, 71(3), 175-193, 2014a.

893 Xia, S., Zhao, Q., Li, B., and Shen, G.: Anthropogenic source VOCs emission inventory of Jiangsu Province (In  
894 Chinese), *Research of Environmental Sciences*, 27(2), 120-126, 2014b.

895 Xu, Z. N., Huang, X., Nie, W., Chi, X. G., Xu, Z., Zheng, L. F., Sun, P., Ding, and A. J.: Influence of synoptic

896 condition and holiday effects on VOCs and ozone production in the Yangtze River Delta region, China,  
897 *Atmospheric Environment*, 168, 112-124, 2017.

898 Xue, L., Wang, T., Louie, P. K., Luk, C. W., Blake, D. R., Xu, Z.: Increasing external effects negate local efforts  
899 to control ozone air pollution: a case study of Hong Kong and implications for other Chinese cities,  
900 *Environmental Science and Technology*, 48(18), 10769, 2014a.

901 Xue, L.K., Wang, T., Gao, J., Ding, A.J., Zhou, X.H., Blake, D.R., Wang, X.F., Saunders, S.M., Fan, S.J., Zuo,  
902 H.C., Zhang, Q.Z. and Wang, W.X.: Ground-level ozone in four Chinese cities: precursors, regional  
903 transport and heterogeneous processes, *Atmospheric Chemistry and Physics* 14, 13175-13188, 2014b.

904 Xue, L.K., Wang, T., Guo, H., Blake, D.R., Tang, J., Zhang, X.C., Saunders, S.M., Wang, W.X.: Sources and  
905 photochemistry of volatile organic compounds in the remote atmosphere of western China: results from the  
906 Mt. Waliguan Observatory, *Atmospheric Chemistry and Physics* 13, 8551-8567, 2013.

907 Xue, L.K., Wang, T., Wang, X.F., Blake, D.R., Gao, J., Nie, W., Gao, R., Gao, X.M., Xu, Z. and Ding, A.J.: On  
908 the use of an explicit chemical mechanism to dissect peroxy acetyl nitrate formation, *Environmental*  
909 *Pollution* 195, 39-47, 2014c.

910 Yuan, B., Chen, W.T., Shao, M., Wang, M., Lu, S.H., Wang, B., Liu, Y., Chang, C.C., Wang, B: Measurements  
911 of ambient hydrocarbons and carbonyls in the Pearl River Delta (PRD), China, *Atmos. Res.*, 116, 93-104,  
912 2012.

913 Yuan, Z., Lau, A. K. H., Shao, M., Louie, P. K. K., Liu, S. C., and Zhu, T.: Source analysis of volatile organic  
914 compounds by positive matrix factorization in urban and rural environments in Beijing, *Journal of*  
915 *Geophysical Research*, 114, D00G15, doi:10.1029/2008JD011190, 2009.

916 Yuan, Z.B., Zhong, L.J., Lau, A.K.H., Yu, J.Z. and Louie, P.K.K.: Volatile organic compounds in the Pearl River  
917 Delta: identification of source regions and recommendation for emission-oriented monitoring strategies,  
918 *Atmospheric Environment*, 76, 162-172, 2013.

919 Zhang, J., Wang, Y., Wu, F., Lin, H., and Wang, W.: Nonmethane hydrocarbon measurements at a suburban site  
920 in Changsha City, China. *Sci. Total Environ.*, 408 (2), 312-317, 2009.

921 Zhang, X., Xue, Z., Li, H., Yan, L., Yang, Y., Wang, Y., Duan, J., Li, L., Chai, F., Cheng, M., and Zhang, W.:  
922 Ambient volatile organic compounds pollution in China, *Journal of Environmental Sciences*, 55, 69-75,  
923 2017.

924 Zhang, Y. L., Wang, X. M., Barletta, B., Simpson, I.J., Blake, D.R., Fu, X.X., Zhang, Z., He Q.F., Liu, T.Y., Zhao,  
925 X.Y., and Ding, X.: Source attributions of hazardous aromatic hydrocarbons in urban, suburban and rural  
926 areas in the Pearl River Delta (PRD) region, *Journal of Hazardous Materials*, 250-251, 403-411, 2013.

927 Zhang, Y. X., An, J. L., Wang, J. X., Shi, Y. Z., Liu, J. D., and Liang, J. S.: Source analysis of volatile organic  
928 compounds in the Nanjing industrial area and evaluation of their contribution to ozone, *Environmental*  
929 *Science*, 39(2), 502-510, 2018.

930 Zhang, Y.H., Su, H., Zhong, L.J., Cheng, Y.F., Zeng, L.M., Wang, X.S., Xiang, Y.R., Wang, J.L., Gao, D.F., Shao,  
931 M., Fan, S.J. and Liu, S.C.: Regional ozone pollution and observation-based approach for analyzing ozone-  
932 precursor relationship during the PRIDE-PRD2004 campaign, *Atmospheric Environment*, 42, 6203-6218,  
933 2008.

934 Zhang, Y.L., Wang, X., Barletta, B., Simpson, I.J., Blake, D.R., Fu, X., Zhang, Z., He, Q., Liu, T., Zhao, X. and  
935 Ding, X.: Source attributions of hazardous aromatic hydrocarbons in urban, suburban and rural areas in the  
936 Pearl River Delta (PRD) region, *Journal of Hazardous Materials*, 250, 403-411, 2013.

937 Zhang, Y.L., Wang, X.M., Blake, D.R., Li, L.F., Zhang, Z., Wang, S.Y., Guo, H., Lee, F.S.C., Gao, B., Chan,  
938 L.Y., Wu, D. and Rowland, F.S.: Aromatic hydrocarbons as ozone precursors before and after outbreak of  
939 the 2008 financial crisis in the Pearl River Delta region, south China, *Journal of Geophysical Research*, 117,  
940 D15306, doi:10.1029/2011JD017356, 2012

941 Zhang, Y.L., Yang, W.Q., Simpson, I.J., Huang, X.Y., Yu, J.Z., Huang, Z.H., Wang, Z.Y., Zhang, Z., Liu, D.,  
942 Huang, Z.Z., Wang, Y.J., Pei, C.L., Shao, M., Blake, D.R., Zheng, J.Y. and Huang, Z.J.: Decadal changes  
943 in emissions of volatile organic compounds (VOCs) from on-road vehicles with intensified automobile  
944 pollution control: case study in a busy urban tunnel in south China, *Environmental Pollution*, 233, 806-819,  
945 2018.

946 Zhao, Q, Shen, G., Li, L., Chen, F., Qiao, Y.Z., Li C.Y., Liu Q., and Han, J.Z.: Ambient Particles (PM10, PM2.5,  
947 and PM1.0) and PM2.5 chemical components in Western Yangtze River Delta (YRD): An Overview of Data  
948 from 1-year Online Continuous Monitoring at Nanjing, *Aerosol Science and Engineering*, 1, 107-118, 2017.

949 Zheng, J. Y., Shao, M., Che, W. W., Zhang, L. J., Zhong, L. J., Zhang, Y. H., and Streets, D.: Speciated VOC  
950 emission inventory and spatial patterns of ozone formation potential in the Pearl River Delta, China,  
951 Environ. Sci. Technol., 43, 8580-8586, 2009.

952 Zheng, J.Y., Yu, Y.F., Mo, Z.W., Zhang, Z., Wang, X.M., Yin, S.S., Peng, K., Yang, Y., Feng, X.Q. and Cai, H.H.:  
953 Industrial sector-based volatile organic compound (VOC) source profiles measured in manufacturing  
954 facilities in the Pearl River Delta, China, Science of the Total Environment, 456-457, 127-136, 2016.

955 Zheng, J.Y., Zhong, L.J., Wang, T., Louie, P.K.K. and Li, Z.C.: Ground-level ozone in the Pearl River Delta  
956 region: analysis of data from a recently established regional air quality monitoring network, Atmospheric  
957 Environment 44, 814-823, 2010.

958 Zhou, D., Li, B., Huang X., Virkkula, A., Wu, H.S., Zhao, Q.Y., Zhang, J., Liu, Q., Li, L., Li, C.Y., Chen, F.,  
959 Yuan, S.Y., Qiao, Y.Z., Shen, G.F., and Ding A.J.: The impacts of emission control and regional transport  
960 on PM<sub>2.5</sub> ions and carbon components in Nanjing during the 2014 Nanjing Youth Olympic Games, Aerosol  
961 and Air Quality Research, 17(3), 730-740, 2017.

962 Zou, Y., Deng, X. J., Zhu, D., Gong, D. C., Wang, H., Li, F., Tan, H. B., Deng, T., Mai, B. R., Liu, X. T., and  
963 Wang, B. G.: Characteristics of 1 year of observational data of VOCs, NO<sub>x</sub> and O<sub>3</sub> at a suburban site in  
964 Guangzhou, China, Atmos. Chem. Phys., 15, 6625–6636, 2015.